UNIVERSITÄT STUTTGART
INSTITUT FÜR STATIK UND DYNAMIK DER LUFT- UND RAUMFAHRTKONSTRUKTIONEN
PROFESSOR DR.-ING. BERND-H. KRÖPLIN

MASTER THESIS

Abdolhamid Attaran

Modeling and Finite Element Simulation of the Viscoelastic Behavior of Dielectric Elastomers

June 2010

PFAFFENWALDRING 27, 70569 STUTTGART

UNIVERSITÄT STUTTGART
INSTITUT FÜR STATIK UND DYNAMIK DER LUFT- UND RAUMFAHRTKONSTRUKTIONEN
Prof. Dr.-Ing. Bernd Kröplin, Pfaffenwaldring 27, D-70550 Stuttgart, Telefon 0711/685-3612, Telefax 0711/685-3706

Master Thesis of Abdolhamid Attaran

Modeling and Finite Element Simulation of the Viscoelastic Behavior of Dielectric Elastomers

Dielectric elastomers (DEs) are smart materials which produce large strains (up to 300%). They belong to the group of electronic electroactive polymers (EAP). Based on their simple working principle, dielectric elastomer actuators transform electric energy directly into mechanical work. DEs are lightweight and have a high elastic energy density.

Working principle:
A dielectric elastomer actuator is a compliant capacitor, where a passive elastomer film is sandwiched between two compliant electrodes. By applying a voltage between the electrodes, an electrostatic pressure (in thickness direction) arises. Due to the mechanical compression the elastomer film contracts in the thickness direction and expands in the plane directions of the polymer film.

Aim of this work to get a detailed understanding of the active behavior of DEs and to develop a numerical model (incl. hyper-viscoelasticity and electro-mechanical coupling).

The work comprises the following items:

- literature review on dielectric elastomers
- introduction to viscoelastic material laws
- development of actuation model
- calibration of the model
- numerical simulation of DE actuator

submission of the thesis: 28.06.2010
supervisors: Dr.-Ing. Thomas Wallmersperger
Prof. Dr.-Ing. habil. Bernd Kröplin

"We are at our very best, and we are happiest, when we are fully engaged in work we enjoy on the journey toward the goal we've established for ourselves. It gives meaning to our time off and comfort to our sleep. It makes everything else in life so wonderful, so worthwhile."

Earl Nightingale

UNIVERSITY OF STUTTGART

Abstract

Master of Science in Computational Mechanics

by Abdolhamid Attaran

Simulation of actuation principles of Dielectric Elastomers (DEs) was sought in this thesis. Of particular interest was the study of the viscoelastic behavior of DEs using the Finite Element Method (FEM). To that end a linear viscoelastic material model was implemented in ABAQUS general purpose Finite Element code as a user material subroutine (UMAT). A model problem based on the work of Wissler [1] was exploited to verify whether the abovementioned UMAT was sufficient to simulate the actuation of a DE. The model used the hyper-viscoelastic material model. To account for the Maxwell stress induced by the electric field, the stress tensor was initiated by a pre-stress. It was concluded, however, that the linear viscoelastic material model was inadequate to simulate DEs and one should use hyper-viscoelastic models to accurately simulate the actuation of DEs. As an enhancement to that, the development of another UMAT based on the work of Zhao and Suo [2] was suggested.

Acknowledgements

First and foremost, I would like to express my deep and sincere gratitude to my supervisors, Prof. Dr.-Ing. habil. Bernd Kröplin and Prof. Dr.-Ing. Thomas Wallmersperger for giving me the opportunity to work in their research team. I will forever be grateful for the guidance, ideas, and encouragement; their excellent supervision has been invaluable.

I am very grateful to European Commission on Training and Education for granting me the Erasmus Mundus scholarship to study Master of Science in Computational Mechanics.

I would also like to thank the administration of the International Master of Science in Computational Mechanics both in Barcelona and Stuttgart for the coordination and support throughout my studies especially Prof. Díez the coordinator of the course, Dr. Rosato, the former coordinator of the COMMAS master program in Stuttgart and Mrs. Zielonka, the secretary of the course in Barcelona.

Last but not least, I thank my family for supporting me in my efforts. This thesis is dedicated to them.

Contents

Abstract ii

Acknowledgements iii

List of Figures vi

List of Tables vii

Symbols viii

1 Introduction 1
- 1.1 General Overview . . . 1
- 1.2 Structure of the Thesis . . . 2

2 Viscoelastic Materials 3
- 2.1 Fundamentals . . . 3
- 2.2 Modeling . . . 5
  - 2.2.1 General Overview . . . 5
  - 2.2.2 Earlier Works . . . 7
- 2.3 Experiments . . . 14

3 Dielectric Elastomers 16
- 3.1 Fundamentals . . . 16
- 3.2 Modeling . . . 19
- 3.3 Experiments . . . 24
- 3.4 Applications . . . 25

4 Modeling of Dielectric Elastomers 26
- 4.1 Introduction to Nonlinear Analysis . . . 26
- 4.2 Nonlinear Continuum Mechanics . . . 27
  - 4.2.1 Continuum Body . . . 27
  - 4.2.2 Deformation Gradient Tensors . . . 28
  - 4.2.3 Strain Tensors . . . 29

4.2.4 The Concept of Stress 30
4.3 Infinitesimal Strain Theory 33
4.3.1 General Overview 33
4.3.2 Voigt-Notation 33
4.3.3 Spherical and Deviatoric Tensors 35
4.4 Balance Laws 35
4.5 Constitutive Equations 38
4.5.1 General Overview 38
4.5.2 3D Formulation of the Viscoelastic Constitutive Model . . . 40
4.5.3 Constitutive Model for Dielectric Elastomers 42
4.6 Finite Element Implementation of Linear Viscoelasticity 44
4.6.1 Finite Element Formulation of a Nonlinear Problem 44
4.6.2 Stress Updates and Constant Tangent Moduli 47
4.6.3 Addition of the Maxwell Stress in the Material Model 49
4.6.4 Implementation of the Algorithm in ABAQUS 49

5 Numerical Simulation of Dielectric Elastomers 51
5.1 General overview 51
5.2 UMAT Verification 51
5.3 Model Problem 54
5.3.1 General Overview 54
5.3.2 Calibrating the Stretch Ratio 56
5.3.3 Test Cases 56
5.3.4 Effect of Varying Applied Voltage on the Activation 57
5.3.5 Application of UMAT 57
5.3.6 Three Dimensional Extension 59

6 Conclusion and Outlook 61

A User Subroutines 63
A.1 UMAT for Representation A 63
A.2 UMAT Developed by Prof. R. M. Hacket 68
A.2.1 UMAT with Two Maxwell Elements (N = 2) 68
A.2.2 UMAT with Four Maxwell Elements (N = 4) 75
A.3 “SIGINI” Subroutine 83

Bibliography 84

List of Figures

2.1 Voigt element 4
2.2 Creep response 4
2.3 Maxwell element 4
2.4 Stress relaxation 4
2.5 Wiechert element 5

3.1 DE actuator in the de-activated (left) and activated state (right) [51] 18
3.2 Different DE configurations: (a) Extenders/Bimorphs, (b) cylindrical actuators, (c) linear actuators, (d) inflatable membranes, (e) annular membranes, (f,g) planar configurations [45]. 18

4.1 Motion of a continuum body 28
4.2 Traction vector 31
4.3 Cauchy's stress tensor components 32
4.4 Material box 39
4.5 Generalized Maxwell model 41
4.6 Out-of-plane pressure p_z and lateral stress p_r acting on the dielectric in a circular actuator, axisymmetric view [1] 44

5.1 Two dimensional model problem [1] 54
5.2 Three dimensional model problem 59
5.3 Activate DE with 3 kV 60

List of Tables

2.1 Material symmetry and the independent material constants 7

3.1 List of the leading EAPs [5] 16

5.1 Material properties for UMAT verification 52
5.2 UMAT verification results 53
5.3 DE properties from a relaxation test [48] 54
5.4 Calibration results of the stretch ratio using the lateral pressure approach 56
5.5 Calibration results of the stretch ratio using pre-stress approach . . 56
5.6 Test cases of Maxwell Stress inclusion in the system 57
5.7 Effect of applied voltage, U, on the elongation of DE 57
5.8 Results of DE actuation simulation with UMAT, ABAQUS Viscoelasticity and ABAQUS Hyper-viscoelasticity 58
5.9 DE material properties for UMAT 58
5.10 Results of 3D DE actuation simulation 59

Symbols

$\boldsymbol{\alpha}_i$	Tensor of internal variables
$\boldsymbol{\beta}_i$	Tensor of external forces
$\partial\Omega$	Surface area of the continuum body
∂_ε	Partial differentiation with respect to ε
∂_θ	Partial differentiation with respect to θ
$\partial_\mathcal{I}$	Partial differentiation with respect to $\mathcal{I}$
ϵ	Eigenvalue
$\boldsymbol{\varepsilon}$	Strain tensor
$\boldsymbol{\varepsilon}'$	Isochoric (Deviatoric) strain tensor
$\boldsymbol{\varepsilon}_s$	Viscous strain
$\boldsymbol{\varepsilon}^p$	Plastic strain
ε_0	Permittivity of free space
ε_r	Dielectric constant
η	Entropy per unit of mass or specific entropy
η_i	Viscosity of the dashpots
θ	Temperature
κ	Bulk modulus
λ_t	Stretch ratio in the thickness direction
λ_p	Pre-stretch ratio
μ_0	Instantaneous shear modulus of the spring in the Maxwell element

μ_∞	Long-term shear modulus of the spring in the Maxwell element
μ_i	Shear modulus of the spring in the Maxwell arm
ν	Poisson's ratio
ξ	Reduced time
Π	Functional
ρ	Density
$\boldsymbol{\sigma}$	Cauchy (true) stress tensor
$\boldsymbol{\sigma}_{esp}$	Spherical stress tensor
$\boldsymbol{\sigma}'$	Deviatoric stress tensor
$\boldsymbol{\sigma}_E$	Elastic stress tensor
$\boldsymbol{\sigma}_M$	Maxwell stress tensor
$\boldsymbol{\tau}$	Kirchhoff stress tensor
τ_i	Relaxation time
$tr[\bullet]$	Trace of a tensor
Ω_t	Configuration at time t (current configuration)
Ω_0	Reference configuration
Ψ	Helmholtz free energy per unit of mass or energy storage function
Φ	Dissipation function
φ	Motion mapping
φ^{-1}	Inverse motion mapping
$\mathbf{B}$	**B**-Matrix
$\mathbf{b}$	Body forces
$\mathbb{C}$	Constant tangent moduli
$\mathbb{C}$	Elasticity tensor
$\mathbb{C}_{ijkl}$	The elastic coefficients
$C_{i\ i=10,20,30}$	Yeoh's model coefficients

$\mathcal{D}_{local}$	The Rate of internal dissipation per unit of spatial volume
$\mathcal{D}_{con}$	The rate of internal dissipation by heat conduction per unit of spatial volume
$\mathbf{d}$	Nodal vector
$d\mathbf{X}$	Material tangent vector
$d\mathbf{x}$	Spatial tangent vector
dL	Material length
dl	Spatial length
$d\mathbf{f}$	Resultant current infinitesimal force
dS	Surface element in reference configuration
ds	Surface element in current configuration
$d\mathbf{f}$	Resultant current infinitesimal Force
$\mathbf{E}$	Green-Lagrange strain tensor
$\mathbf{e}$	Euler-Almansi strain tensor
e	Volumetric strain
e	Internal energy per unit of mass
$e_{i\ i=1,2,3}$	Unit vector
E	Internal energy
E	Young's modulus
$\tilde{E}$	Electric field
$\mathcal{F}$	External forces/Resultant forces acting on the material volume
$\mathbf{F}$	Deformation gradient tensor
$\mathbf{F}^{-1}$	Inverse deformation gradient tensor
$\mathbf{f}_{int}$	Internal forces
$\mathbf{f}_{ext}$	External forces
G	Shear modulus
$\bar{g}_i^p$	Dimensionless shear modulus

H	Entropy
$\mathbf{H}$	History of internal variables/forces
$\mathbf{I}$	Second-order identity tensor
$\mathbb{I}$	Fourth-order identity tensor
$\mathcal{I}$	Generalized vector of internal variables
K	Kinetic energy
$\bar{k}_i^p$	Dimensionless bulk modulus
$\mathbf{K}$	Tangent Stiffness matrix
$\mathbf{M}$	Momentum
$\mathbf{M}_L$	Linear momentum
$\mathbf{M}_O$	Angular momentum with respect to O
$\mathbf{N}$	Unit normal vector in reference configuration
$\mathbf{N}(\mathbf{u})$	Shape function
$\mathbf{n}$	Unit normal vector in current configuration
$\mathbf{P}$	First Piola-Kirchhoff (nominal) stress tensor
P_{ext}	External mechanical power
P	Maxwell pressure
$\mathbb{P}$	Fourth-order deviatoric projection tensor
Q_{ext}	External thermal power
$\mathbf{q}$	Spatial heat flux per unit of spatial surface area
$\mathbf{r}$	Residuum vector
$\mathbf{r}$	Distance vector
r	Internal hear source rate per unit of mass
$\mathbf{S}$	Second Piola-Kirchhoff stress tensor
t	Time
$\mathbf{t}$	Cauchy (true) traction vector
$\mathbf{T}$	First Piola-Kirchhoff (nominal) traction vector
$\mathbf{u}$	Displacement field (tensor)

U	Applied voltage
v	Volume
$\mathbf{v}$	Velocity vector
$\mathbf{X}$	Position vector in reference configuration
$\mathbf{x}$	Position vector in current configuration
z	Current Dielectric Elastomer's thickness
z_0	Initial Dielectric Elastomer's thickness

Dedicated to my beloved parents and sister

Chapter 1

Introduction

1.1 General Overview

Dielectric Elastomers (DEs) have recently gained an unprecedented popularity to be used as actuators replacing their own bulky traditional counterparts. One area which benefits the most from such actuators is the field of imitating biology known as biomimetics [3] where DEs can be served as artificial muscles. This is in part due to DEs' low density ($\rho \approx 900 - 1500$ kg/m^3) which matches that of human muscle [4].

Dielectric Elastomer Actuators (DEAs), however, are still at their early stage of development and there is an ever increasing demand for both experimental and computational investigations to address the potential problems associated with such actuators. Of particular interest is to examine efficiency, functionality, and precision of these materials [3]. This requires the progress in such fields as related computational chemistry models, comprehensive material science, electromechanics analytical tools, improved material processing techniques, viscoelasticity of solids and control theory [5].

The motivation behind the present study stems itself from the growing demand of numerical techniques to model and simulate the mechanical behavior of DEs. Being a multifield problem, modeling and simulation of such materials is rather complicated and only a few works are available. Of particular interest is to examine the viscoelastic behavior of DEAs using Finite Element Method. This work is primarily based on the findings of Goulbourne et al. [6] and Wissler [7].

The primary objective of the present study is to create the necessary tools for modeling and simulation of the actuation principles of DEs and to create the necessary platform for further investigations in this field. The scope of the work, however, is limited to study the viscoelastic behavior of DEs. To that end the constitutive equations of a viscoelastic solid will be implemented and then the mechanical stress will be augmented by a Maxwell stress as stated by Goulbourne et al. [6]. Study the effects of nonlinearities on the behavior of the mechanical response is also sought through the considerations of geometrical and material nonlinearities.

1.2 Structure of the Thesis

The first chapter is intended to present an introduction to the work followed by objectives and scope of the work. Chapter two discusses the fundamentals of viscoelasticity and some modeling aspect of this subject. This chapter concludes with a rather brief review of the works available in the literature on the subject of viscoelasticity. Chapter three is completely devoted to the introduction of DEs including fundamentals, modeling and the review of the existing works on modeling DEs in literature. This chapter is wrapped up with some applications and experimental aspects of DEs. The related theories are presented in chapter four and chapter five is devoted to the results of the study followed by a discussion on the obtained results. This thesis is concluded in chapter six including some remarks on the possible future extension.

Chapter 2

Viscoelastic Materials

2.1 Fundamentals

In this section a basic overview of viscoelastic materials will be presented. Such materials as elastomers [8], rubbers, fibers, plastics, leathers, glasses, muscle tissues, wood [9], and building materials such as concrete [10] exhibit a time dependent mechanical behavior called viscoelasticity where the material response is not only dependent on the current state of deformation but also on the whole deformation history [11]. The present work, however, is only concerned with the viscoelastic behavior of DEs.

In experiment with these materials one can observe the following basic effects [8]: (1) creep under constant load, (2) stress relaxation under constant deformation, and (3) delayed strain recovery on unloading.

The researches on viscoelasticity were initiated by physicists such as Maxwell, Boltzmann, Voigt, and Kelvin in the nineteenth century [12]. While the classical linear theory was first presented by Boltzmann in 1874 [13], Maxwell suggested the superposed elastic-viscous formulation for the stress relaxation with constant strain and Voigt introduced a similar formulation but for creep under constant stress [9]. These formulations correspond to mechanical models (mechanical analogues [8]) consisting of a spring and a dashpot. If these elements are connected in series, it is called Maxwell element (Fig. 2.3 and Fig. 2.4), whereas placement of the spring and dashpot in parallel forms the so-called Voigt element [9] (Fig. 2.1 and Fig. 2.2).

As stated by Tobolsky and Andrews [9] it is apparent that both models are not complete in describing the material behavior. While Maxwell element fails to describe the creep, Voigt element is not able to consider the stress relaxation. This has led to the introduction of the Wiechert's mechanical model (Generalized Maxwell-element [14]) which is a larger number of Maxwell elements placed in parallel. This is illustrated in Fig. 2.5.

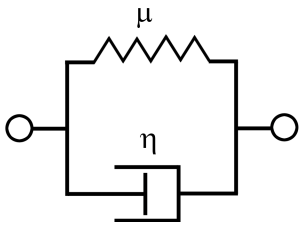

FIGURE 2.1: Voigt element

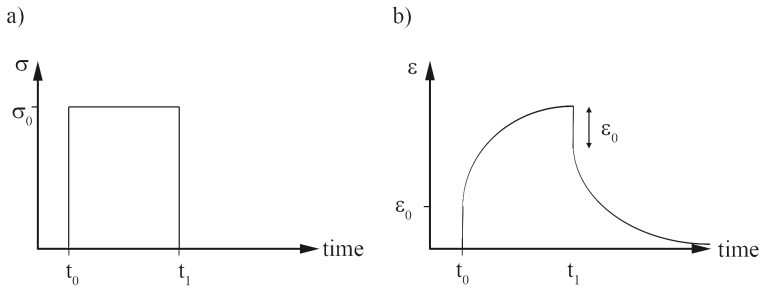

FIGURE 2.2: Creep response

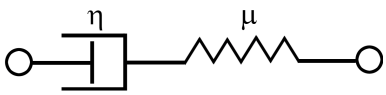

FIGURE 2.3: Maxwell element

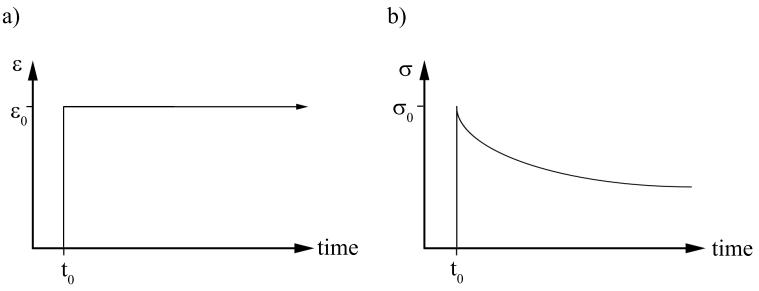

FIGURE 2.4: Stress relaxation

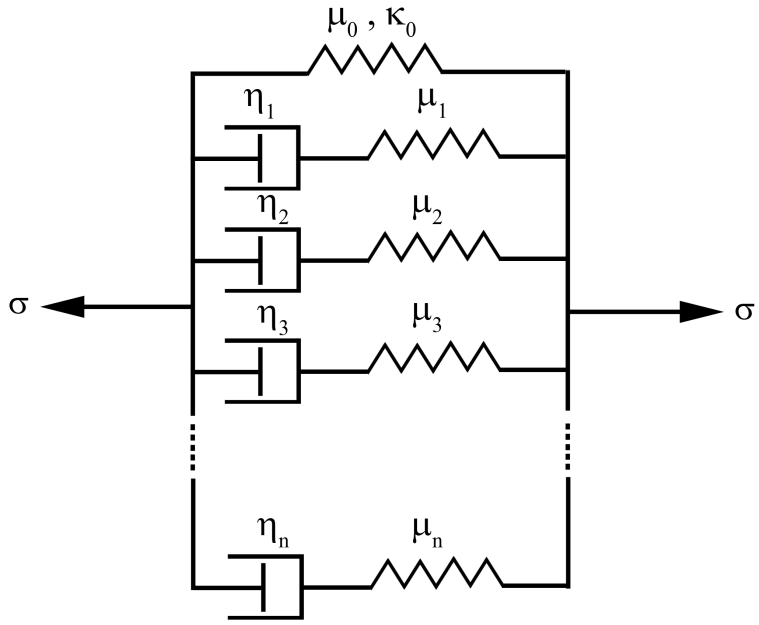

FIGURE 2.5: Wiechert element

2.2 Modeling

2.2.1 General Overview

The term modeling here is referred to as the determination of a stress-strain relationship also known as the constitutive law[1] in viscoelastic materials. It also accounts for using this relationship in conjunction with the governing equations to determine the stresses and deformations in structures made of these materials [8].

As viscoelastic materials with time dependent mechanical behavior began to emerge, it was evident that the existing classical theories were definitely insufficient to describe the stress-strain relationships in such materials [9]. Ever since, all the efforts have, therefore, been centered around finding a constitutive law which accurately predicts the mechanical response of viscoelastic materials [8].

In developing the constitutive equations, one should consider whether the response is linear or nonlinear. Linear assumptions are only applicable for materials experiencing small strains, i.e. when the magnitude of the strain has been small for all past times ($|\varepsilon(s)| \leq 1, \forall\ s \in (-\infty, t]$) [8]. Nonlinearity in viscoelastic response, on

[1]The constitutive equations discussed here are phenomenological rather than molecular in origin. These forms of equations arise from mathematical assumptions about the mechanical response rather than assumptions about molecular mechanisms underlying that response [8].

the other hand, occurs when there is large deformation and/or non-linear material properties [8]; it is clear though that the linear theories are inadequate to describe such responses of viscoelastic materials.

The derivation of linear viscoelastic constitutive equations is straightforward by using either the consequences of linearity or mechanical analogues as stated in the previous section (Generalized Maxwell-element) [8]. In the first approach also known as the frequency domain approach [11], a complex structural problem in linear viscoelasticity is solved using the correspondence principle between elasticity and viscoelasticity. Based on the *Laplace* transformation, the viscoelastic problem is turned into an associated elastic counterpart. After the elastic problem is solved, the solution to the original problem is obtained by performing the numerical *Laplace inverse* transformation. The problem of this approach though is that it is difficult to be extended to nonlinear problems.

In the second approach also known as the time domain approach [11], by the virtue of the incremental finite element method, the incremental equations are formulated, and the problem is eventually solved step-by-step. Because a recursive form of constitutive equations is used, this approach saves much computer storage, as compared with the Laplace inverse transformation and can easily be extended to nonlinear problems.

There is, on the other hand, no generally accepted well-defined form for the constitutive equations for nonlinear viscoelastic solids [8]. Nonetheless there are some theories which can be used to establish the constitutive laws for nonlinear viscoelastic solids; among others are, rate and differential type constitutive equations, Green-Rivlin multiple integral constitutive equation, finite linear viscoelasticity, Pipkin-Rogers constitutive theory, quasi-linear viscoelasticity, and K-BKZ constitutive theory [2] [8].

Other considerations in determination of the constitutive equations are the material symmetry restrictions and compressibility of the materials [8]. Assuming to be incompressible, material symmetry restriction means whether the material is isotropic, transversely isotropic, orthotropic, or fully anisotropic. In a fully anisotropic case, there are 21 independent material constants in the elasticity tensor. This number reduces to 9 for orthotropic materials while there are only 5 independent constants in the case of transversely isotropic materials. An isotropic

[2]Proposed by Kaye [15], Bernstein, Kearsley, and Zapas [16]

material has only 2 independent material constants. This has been summarized in Table 2.1.

TABLE 2.1: Material symmetry and the independent material constants

Material Symmetry	**Independent Material Constants**
Fully Anisotropyic Materials	E_x, E_y, E_z; $\nu_x, \nu_y, \nu_z, \nu_{\perp xy}, \nu_{\perp xz}, \nu_{\perp yz}, \nu_{\parallel xy}, \nu_{\parallel xz}, \nu_{\parallel yz}$; $G_x, G_y, G_z, G_{\perp xy}, G_{\perp xz}, G_{\perp yz}, G_{\parallel xy}, G_{\parallel xz}, G_{\parallel yz}$ Total number: 21
Orthotropic Materials	E_x, E_y, E_z; $\nu_{xy}, \nu_{xz}, \nu_{yz}$; G_{xy}, G_{xz}, G_{yz} Total number: 9
Transversely Isotropic Materials	$E_x, E_z, \nu_x, \nu_z, G_{xz}$ Total number: 5
Isotropic Materials	E & ν Total number: 2

In the following some earlier works on modeling the viscoelastic materials are briefly reviewed.

2.2.2 Earlier Works

One of the earliest studies on modeling viscoelastic behavior of materials traces back to 1945 when Tobolsky and Andrews [9] exploited a molecular approach to describe the mechanical behavior of materials for which the classical theories of solid mechanics and fluid mechanics were insufficient. Their attention was mainly given to the rubberlike materials. They performed series of creep and relaxation tests to validate their theoretical approach. Through these experiments they observed three regions of stress-temperature-time dependence; namely, a low, an intermediate and a high temperature region and discussed the creep and relaxation mechanism in each of these regions from a molecular point of view.

Later on, Read [17] presented his method of stress analysis for compressible viscoelastic materials in 1950. In his approach he used Fourier integral and operator methods to demonstrate that elasticity theory could be further extended to account for time-dependent mechanical behavior of isotropic materials. According to him his method was easily extendible to the fully anisotropic case.

In 1956, Lee [18] published a paper which was mainly concerned with the stress analysis of linear viscoelastic materials such as polymers and plastics. In this paper

he talked about three major problems in developing any method of stress analysis; namely, (1) finding the properties of material, (2) deciding on the suitable model or operator, and (3) analyzing the stress distribution. He adopted the quasi-static method for his work although he finally argued that there were some limitations associated with this method.

Motivated by the challenging mathematical problems and the increasing use of inelastic materials, Lee [19] proposed another method of stress analysis of viscoelastic materials. He used the operator relations to represent a given viscoelastic body just two years after he published his paper on stress analysis of linear viscoelastic materials [18]. He asserted that either differential or integral operator relation between stress and strain was more convenient, whereas the integral operators were more convenient for relaxation and creep functions.

In line with the development in nonlinear continuum mechanics in early 1960s, Coleman and Noll [20] proposed the fundamental assumptions of linear viscoelasticity. They first presented the theory of infinitesimal viscoelasticity based on the assumption that at microscopic level the substances could be regarded as spring and dashpots connected in a complex network. This assumption could make the formulation of the theory simple since it considered the smoothness at macroscopic level. To characterize the smoothness they introduced the history of deformation, and to measure the level of smoothness they defined a norm indicating how two histories were close to each other. Further in their work, by the help of the theory of nonlinear continuum mechanics they presented the theory of finite linear viscoelasticity and treated the classical infinitesimal viscoelasticity as a special case. They contented, however, that these two theories had one fundamental difference; the infinitesimal theory was not physically meaningful since it did not include the basic ingredients required for material objectivity; i.e. invariants. Conversely the finite linear theory contained these basic ingredients, hence could be used for finite deformations.

Meanwhile, Pipkin [21] suggested some nonlinear integrals and argued that under proper assumptions, the approximation of these integrals provided the basic constitutive law for small deformations of viscoelastic solids. To that end he considered conditions where the deformation was small but finite for materials with memory. Based on the work of other researchers (Green and Rivlin [22]; Noll [23]), he reviewed the derivation of these nonlinear integrals which were relating stress

and strain. He also asserted that the assumption of isotropy or incompressibility made these integral relatively simple.

In 1968, Zienkiewicz and co-workers [24], developed a general numerical procedure to solve a broad-class of viscoelastic problems of the quasi-static type. Their research was mainly concerned with the creep analysis in the field of concrete technology and rock mechanics. In their work, they demonstrated how to extend such numerical methods as the finite element method applicable to elastic problems to account for viscoelasticity. They exploited Kelvin-Voigt elements to represent the material behavior. They asserted that this method was suitable for computational purposes. Next, they validated their approach against the exact solution of viscoelasticity and tested the rate of convergence of their methods of solution. They finally argued that the main obstacle of the future research would be the insufficient physical data regarding the material behavior.

Two years later, Taylor et al. [25] proposed a numerical procedure to solve linear viscoelasticity problems where thermal effects were also included. This algorithm stemmed from a finite element discretization to a set of simultaneous linear integral equations. They asserted that exclusion of the temperature history would result in a set of Volterra integral equations which could be treated using integral transform method, while by the inclusion of temperature history these equations were solved using a step-forward integral procedure. Being computationally inefficient, they adopted an alternative scheme to solve the latter case where the kernel functions of the integral equations were presented by this series:

$$K(\xi - \xi') = \sum_{i=1}^{I} K_i \; f_i(\xi) \; g_i \; (\xi') \tag{2.1}$$

where ξ is the reduced time, $\xi' = \xi(t')$, and f_i and g_i were the elements of the a complete set.

To conclude their work, Taylor and co-workers investigated the validity of their proposed algorithm by applying it to a thermal plane-stress analysis of a thin-walled cylinder.

In the meantime, Pipkin and Rogers [26] suggested an integral series representation of nonlinear viscoelasticity. Prior to their work most of the researches were based on the multiple integral representation suggested by Green and Rivlin in 1957. They contended, however, that this kind of representation posed such problems

as (1) the difficulty of stress and deformation analysis, (2) major experimental difficulty, and (3) possessing no inherent meaning independent of the choice of strain measure, when there was a strongly nonlinear viscoelastic response. Their model was believed to solve or improve the aforementioned problems. In order to consider strong nonlinearity as simple as possible, the first term in their integral series representation was a single integral with a nonlinear integrand. In addition, they arranged the series in such a fashion that the experimental data could be used directly. This was to make the experimental determination of material characteristics simpler.

Schapery [27] proposed a three-dimensional nonlinear constitutive model which was in particular consistent with the nonlinear responses of some metals and plastics in 1969. To that end he discussed certain methods of characterizing nonlinear viscoelastic solids, i.e. developing constitutive relations based on the thermodynamic principles, and using experimental data as an assessment tool for the material properties. The experiment consisted of uniaxial loading under fixed environmental conditions and the influence of the factors such as temperature, humidity, and aging.

Partom and Schanin [28] presented a nonlinear viscoelastic model based on the general Maxwell model with linear springs and nonlinear dashpots. Despite the two already existing integral representations of nonlinear viscoelasticity (multiple and single integral representations), their approach was based on the evolution of the stresses as the internal state variables. They applied this approach to predict the response of various uniaxial loadings and the creep problem of a clamped beam. Using the obtained results, they validated the model. They finally suggested this procedure was simple and straightforward.

One year later, in 1984, Keren et al. [29] developed a two dimensional axisymmetric finite difference code based on the nonlinear viscoelastic procedure developed in Ref. [28]. Their test case was a thin disc glued between two rigid metal anvils loaded in axial direction. With this test case they demonstrated that it was impossible to correctly predict the response of the specimen with linear viscoelastic model.

Another approach to nonlinear viscoelasticity was depicted by Rendell et al. [30] in 1987 based on the "coupling model" of relaxation. Coupling model, as they explained, had the proven potential to relate the features observed in nonlinear

viscoelastic experiment to molecular motions. Giving a brief review of the previous works in the field, they asserted that the nonlinear viscoelasticity models for glassy polymers should meet the following requirements:

1. to be dependent on stress or strain history,
2. to have a constitutive equation non-separable in stress or stress and time,
3. to have a physical meaning for all the parameters,
4. to allow for assessment of material structure toward equilibrium,
5. to predict $\sigma(t)$ and $\varepsilon(t)$ for a variety of stress and strain histories,
6. to predict the dependencies on all physical variables,
7. and to be consistent with the linear models.

They concluded that the simulations using this model revealed many of the important features. These features were also observed experimentally for various strain histories. As an extension of their work, they suggested the inclusion of more complicated conditions such as fatigue and multiaxial experiments.

Gramoll et al. [31] developed a numerical procedure to solve nonlinear viscoelastic problems of orthotropic materials such as fiber-reinforced plastics (FRP) laminated composites. Exhibiting strong time-dependency, the classical lamination theory also known as CLT was clearly not sufficient to accurately predict the evolution of strains and stresses over the time. Making use of the modified Kelvin elements, they included the nonlinearity in the model. They exploited an implicit solution scheme to solve the differential equations that modeled each of the Kelvin elements. They finally used the Newton-Raphson method to solve the resulted simultaneous nonlinear equations. This choice of solution schemes, therefore, led to an unconditionally stable numerical procedure. Gramoll and co-workers later calibrated their predictions using their proposed method with a number of actual experimental tests.

In the beginning of the 1990s, Krishnaswamy et al. [32] presented a finite element algorithm being able to describe both linear and nonlinear viscoelastic material response. In particular, they intended to examine the deformation and failure behavior of such materials. According to them this algorithm was suitable for

analyzing the time-dependent behavior of cracks in viscoelastic materials. They contended the differential representation was much easier to include the nonlinear effects in the formulation of viscoelastic material model. As such, they exploited the differential representation of viscoelastic materials instead of the integral representation in the development of this algorithm. Having verified their algorithm for the case of a uniaxial tensile specimen and an infinite plate with a hole subjected to a remote uniaxial stress, Krishnaswamy and co-workers, then, used this algorithm for stress and strain field determination near the crack tip of a moving crack tip.

Motivated by the increasing application of polymers in engineering, Losi and Knauss [33] addressed the problem of transient and residual stresses in structural parts in a paper published in 1992. This problem was due to the formation of such structural parts at high temperature and cooling below the glass transition temperature. This in conjunction with the associated heat flow and inhomogeneous temperature fields led to the development of residual stress. They discussed the aforementioned problem from a thermorheological point of view and examined their proposed methodology using an infinite cylinder and in a sphere for three constitutive models with different accuracy; namely, the "elementary" model, the "thermorheological" model, and the "semi-elementary" model. They, finally demonstrated that using their procedure, the residual stresses could be higher than an elastic analysis and, thus, the "stress-free temperature" was found to be dramatically above the glass transition.

Ghazlan et al. [34], on the other hand, developed a complete general formulation of linear viscoelastic creep model. This model could easily be extended to deal with such complex viscoelastic problems as aging materials, thermoviscoelastic and dynamic analysis. The primary objective of their proposed model was tackling the computer storage problem of the stress history. To this end they based their model on a discrete creep spectrum[3] and an incremental constitutive equation. Deriving the finite element formulation of the governing equations from the principle of virtual displacements, they demonstrated the functionality of their proposed numerical procedure through a plan-stress plate, a steady-state harmonic oscillation, a circular cylindrical shell, and a spherical shell.

Zaoutsos et al. [35] proposed a material model describing the nonlinear viscoelastic response of unidirectional carbon-fiber-reinforced polymer (FRP) composites.

[3] A finite serries of Kelvin elements coupled with an elastic and viscous response [34].

They modified the Schapery's nonlinear viscoelastic model by adding a viscoplastic term, and determined the nonlinear viscoelastic parameters using a new data-reduction method. These nonlinear parameters were introduced in the creep/recovery of FRP. Zaoutsos and co-workers, finally, validated their proposed method through an experiment.

At the same time, Kaliske and Rothert [14] suggested a linear viscoelastic approach at small and finite strains. They presented the mixed finite element formulation of their proposed numerical procedure for time-dependent deformations of rubber-like structures. They, additionally, discussed such experimental aspects of viscoelasticity as time-temperature superposition principle, WLF-equation, and master curves along the parameter identification in viscoelastic problems.

Motivated by the short coming in addressing the general problem of full thermo-mechanical coupling, large deformation and larger deviations away from thermodynamic equilibrium in earlier researches, Reese and Govindjee [36] proposed a model for finite thermo-viscoelasticity in 1998. According to them this model was physically reasonable and numerically tractable. They asserted, however, that this model yielded results which were more qualitative than quantitative due to the lack of thermo-mechanical coupling experimental results. The development of their numerical procedure was based on the assumptions of (1) multiplicative split of deformation gradient into elastic and inelastic parts, and (2) additive split of Helmholtz free energy into equilibrium and non-equilibrium parts.

Deriving the constitutive relations utilizing the Clausius-Duhem inequality, Reese and Govindjee used an efficient predictor-corrector algorithm to integrate the evolution equation of the constitutive relations and solved the respective initial boundary value problem using a nonlinear finite element method. They, ultimately, applied their procedure to examples of a shear test, and bearing, to demonstrate "physically interesting thermo-mechanical coupling effects" and to prove the robustness of their finite element formulation. They, however, emphasized the need for more efficient solution techniques for three dimensional cases and suggested such techniques as indirect solvers or domain decomposition.

Circular areas like notches and cracks where stress concentrations were likely to happen, as well as the existence of a process (failure) zone around the crack tip are among the sources of nonlinearities in structures made of polymers [37]. By virtue to this fact, Masuero and Creus [37], proposed a finite element algorithm based on

Schapery's nonlinear viscoelastic formulation for fractures and verified their suggested algorithm through three cases of uniaxial tensile specimen, hollow cylinder under internal pressure, and hollow cylinder with radial temperature distribution under pressure. They also discussed the possibility of modeling improvement by introduction of nonlinearity in the process zone through a damage mechanism.

Recently Drapaca et al. [38] and Wineman [8] published two separate review papers discussing the nonlinear constitutive laws in nonlinear viscoelasticity. Presenting a complete overview of the linear constitutive equations, Drapaca et al. were aimed at providing a review of the classical representation of constitutive laws for nonlinear viscoelastic materials and a unified continuum mechanics formulation. Wineman, on the other hand, intended to review all the aspects of modeling in viscoelastic material from a phenomenological point of view. Starting from some historical perspective and presenting the derivation of constitutive equations for linear viscoelasticity using different approaches, Wineman concluded that there was no generally accepted well-defined form for the constitutive equations for nonlinear solids as there was for linear viscoelastic solids. He, however, included some the more well-known nonlinear constitutive equations such as Green-Rivlin multiple integral constitutive equations, finite linear viscoelasticity, Pipkin-Rogers constitutive theory, etc.

2.3 Experiments

In this section a very brief overview on experimental procedure is presented. This section is by no means complete and interested readers are referred to the classical texts on viscoelastic materials such as [39] for a comprehensive overview of the subject matter.

Experimental procedures for viscoelastic materials are similar to experimental procedures in any other branches of mechanics and include load application, measuring, strain and displacement, and transient behavior identification [39]. As explained in Sec. 2.1 while performing such procedures one can observe such phenomena as creep, stress relaxation, and delayed strain recovery on unloading. In the following the first two phenomena are elaborated in more details.

Creep experiments as the simplest method in experimental viscoelasticity is carried out by applying constant stress using deadweight over a sufficiently long

period of time and at elevated temperature [39]. The material responds to the stress with a strain that increases until failure [40]. Viscoelastic creep data can be presented by plotting the creep modulus (constant applied stress divided by the total strain at a particular time) as a function of time. The creep response of a viscoelastic material is illustrated in Fig. 2.2 [41]. Slope of the creep curve at any point is called creep rate. If the specimen under the test is not failed the creep recovery may be measured [42].

Stress relaxation test, on the other hand, is based on the relief of stress under constant strain [42]. Such test is performed on a deformed specimen and the decrease in stress is recorded over a prolonged period of time and at constant elevated temperature. In this case the stress is plotted as a function of time as portrayed in Fig. 2.4.

Chapter 3

Dielectric Elastomers

3.1 Fundamentals

Dielectric Elastomers (DEs) belong to a broad class of smart materials known as electroactive polymers (EAPs). Smart materials are best described as the materials which can detect changes, decide in a rational manner, and act as required in a controlled fashion [3]. EAPs include [3] piezoelectric, electrostrictive, ionic and conductive polymers, elastomers, polymeric blends, electroactive foams and electrorheological fluids. They generally respond to external stimuli in the form of an electric charge or mechanical deformation. These responses are called "sensor effect" and "actuator effect", respectively.

EAPs can also be categorized based on their activation mechanism, i.e. ionic and electronic [5]. Table 3.1 adopted from Ref. [5] presents the leading EAPs. For a detailed explanations on each one of these materials, their history, current status and applications please refer to Ref. [43].

Table 3.1: List of the leading EAPs [5]

Electronic EAP	**Ionic EAP**
Dielectric EAP	Carbon Nanotubes (CNT)
Electrostrictive Graft Elastomers	Conductive Polymers (CP)
Electrostrictive Paper	ElectroRheological Fluids (ERF)
Electro-Viscoelastic Polymers	Ionic Polymer Gels (IPG)
Ferroelectric Polymers	Ionic Polymer-Metal-Composites (IPMC)
Liquid Crystal Elastomers (LCE)	

Operating under the so-called "dry operation" condition, Electronic EAPs can easily be commercialized and their simple fabrication process and longer lifetime is guaranteed [44]. They, however, require a higher actuation voltage than ionic EAPs of about 2 kV [45].

Used as the base material in the present study, DEs are electronic EAPs which deform extensively in the presence of an electric field and can hence be used as actuators in adaptive structures. DEs are capable of about 100% deformation upon activation [45]. The most common DEs are Acrylic elastomers (e.g. 3M VHB series) and silicone (e.g. Nusil R31-2186 or CF 19-2186; Dow Corning HS III RTV) [46, 47]. Example of applications of DEs as actuators include [3, 46–48]: micro air vehicle, flat panel loudspeakers, video displays, haptic devices, disk drivers, mobile mini- and micro-robot, micropumps and microvalves. For a more complete list of applications please refer to the review paper of Biddiss and Chau [46].

Sandwiched between two compliant electrodes[1], operational principle of DEs is as simple as attracting opposite charges and repelling like charges by applying a voltage [46] and returning to its original shape upon removal of the voltage [50]. The electrostatic attraction induces the Maxwell stress which ultimately causes the elastomer to contract in thickness direction and expand in its in-plane direction [51]. Due to the repulsion of like charges on the electrode surface there is an electrical traction [6] caused by the tensile and compressive forces [46]. This traction commonly referred to as electrostatic pressure [48] relates the permittivity of free space, ε_0, the relative permittivity or dielectric constant of the polymer, ε_r, and the applied electric field. Owing to voltage, U, across the elastomer thickness, z; this pressure can be written as [46]:

$$P = \varepsilon_0 \varepsilon_r \left(\frac{U}{z}\right)^2 \tag{3.1}$$

Figure 3.1 demonstrates the actuation principle of a DE.

Based on their required application, DEs come into variety of shapes [45] such as: inflated membrane (circular) configuration, cylindrical configuration, annular configuration, and planar configuration. Figure 3.2 illustrates these configurations [45].

[1]They are called compliant since they allow the dielectric to deform without affecting its mechanical performance [49].

To improve their performance i.e. strain achieved upon actuation for a given voltage, DEs are generally biaxially or uniaxially pre-stretched to reduce the initial film thickness and increase electric field, $\tilde{E}(= U/z)$ [47]. This can also enhance the effective compressive modulus of DEs [47]. On the other hand, pre-stretching reduces actuator power density and the ease of fabrication, increases the risk of stress concentrations and stiffens the material and deteriorates the strain response [46].

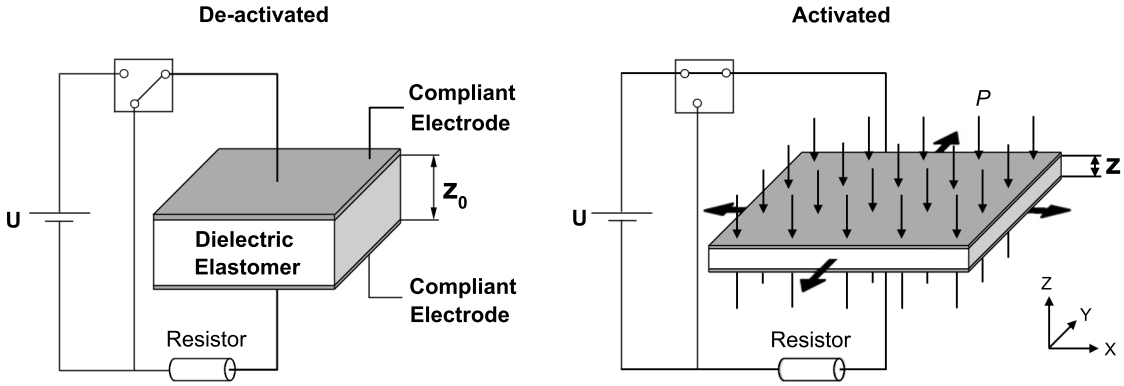

FIGURE 3.1: DE actuator in the de-activated (left) and activated state (right) [51]

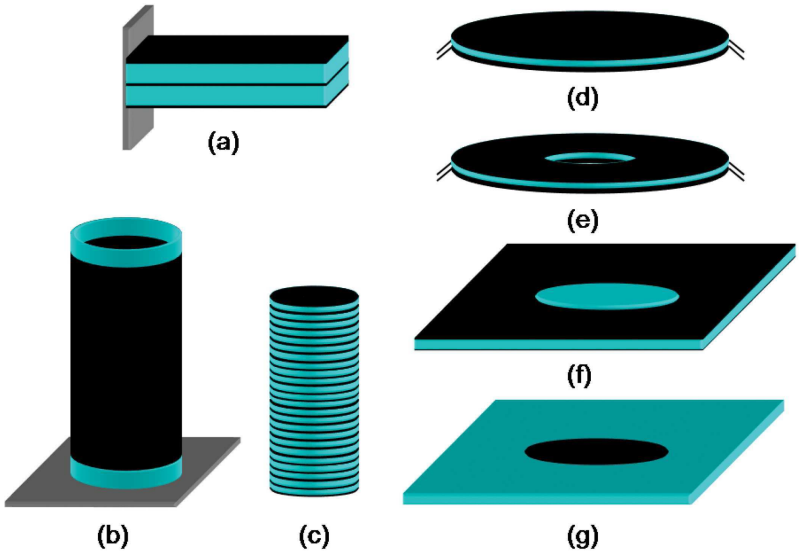

FIGURE 3.2: Different DE configurations: (a) Extenders/Bimorphs, (b) cylindrical actuators, (c) linear actuators, (d) inflatable membranes, (e) annular membranes, (f,g) planar configurations [45].

3.2 Modeling

In Sec. 2.2.2 the general framework for modeling viscoelastic materials was laid out. In this section the attention is primarily given to modeling the activated DEs, whereby the electrical properties of DEs is added to the abovementioned framework. The main challenge here is how to treat the electromechanical coupling. Unlike the electrostatic effects in piezoelectric and electrostrictive materials where the elastic stress depends on the electric field variables, for DEs the Cauchy (true) stress tensor, $\boldsymbol{\sigma}$, is assumed to be the sum of the local elastic stress, $\boldsymbol{\sigma}_E$, and the Maxwell stress, $\boldsymbol{\sigma}_M$, [6]:

$$\boldsymbol{\sigma} = \boldsymbol{\sigma}_E + \boldsymbol{\sigma}_M \tag{3.2}$$

In the following a brief review of the previous works on modeling DEs will be presented where constitutive modeling, electromechanical coupling and some experimental aspects will be discussed.

In order to minimize such limitations as weight, size, complexity and durability associated with the current artificial blood pumps, Goulbourne and co-workers [6] sought to incorporate electroactive material in these devices. To that end, they developed a method for modeling DEs membrane that included both material and geometrical nonlinearities. They exploited the theory of elasticity and electrostatic theory to describe the mechanical and electrical parts of their model, respectively.

Assuming hyperelastic behavior of DEs, they contended that the stress field was simply an augmentation of the elastic Cauchy stress in the presence of the electric field, see Eq. (3.2). Additionally, the boundary of the dielectrics in the presence of conductors was under electrical tractions. In their approach, they modeled the DE as a circular axisymmetric membrane subject to both mechanical forces and traction causing by an electric field. The membrane was pre-stretched and clamped at its edges. Their results showed that the increase in applied voltage would cause an increase in volume and despite the dielectric elastomer actuators' capability in large deformations, their electrical pressure output was very low.

Unlike Goulbourne et al., Wissler and Mazza [48] presented a procedure for finite element modeling and simulation of Dielectric Elastomer Actuators (DEAs) which treated the problem as fully uncoupled. They asserted that two main obstacles in

Finite Element (FE) modeling and simulation of electroactive polymers presented themselves as the actuation modeling and the proper definition of the constitutive equation. Although the presence of electrical field would lead to electromechanical coupling, their approach was to solve the problem as fully uncoupled, simplifying it to a pure mechanical problem.

Using acrylic elastomer VHB 4910 (3M) as the base material for dielectric elastomer, their research work was a combination of experiments and finite element modeling of a biaxially pre-strained actuator. They first performed series of experiments such as relaxation test, tensile test and circular strain test, the result of which were later employed to validate the numerical calculations. In their work large strain response was modeled using strain energy potential of Yeoh [52] and the so-called Prony series to describe the time dependence of the mechanical response. The outcome of their work demonstrated a good agreement between FE calculation and experiment and highlighted the importance of multi-axial testing in determining the proper constitutive models for DEs. Finally, Wissler and Mazza pointed out that main drawback of their proposed procedure was the treatment of the problem as an uncoupled problem where the voltage was incorporated as the output of the calculation.

In the meantime, Kofod and Sommer-Larsen [4], reviewed the present situation in the theory of DEAs aiming at providing an insight into the actuation models and electromechanical coupling background. They proposed non-linear high-strain model requiring only elastic stresses and Maxwell stresses and wrapped up their review with some comments on the improvement of DEs.

Choi et al. [53] proposed a new biomimetic DEAs design called ANTLA (ANTagonistically driven Linear Actuator) with such applications as earthworms or maworms when used as a microrobot. Using these actuators they were seeking to achieve four typical states of human muscles; namely, forward, backward, highly compliant and highly stiff. Satisfying major features of a muscle-like actuator i.e. bidirectional actuation and compliance controllability, their proposed design was composed of a prestretched elastomer film foiled on the frame, which was engaged with uniform pretension along the direction of actuation. Modeling both statically and dynamically, Choi and co-workers applied their design to a prototype aiming at verifying the effectiveness of the modeling techniques as well as the control method. They finally argued that by changing some parameters, their presented idea could result in a paradigm of design in robotics.

Motivated by the increasing interest in using the electromechanical devices based on polymer coated with compliant electrodes, Begley et al. [54] investigated, both theoretically and experimentally, the coupling electrical input and out-of-plane behavior of silicon-based multilayered DEAs in 2005. Their work was aimed at providing (1) "experimental validation of constitutive theories for cracked laminates", (2) "experimental validation of closed form membrane load-deflection solutions that involved strain", and (3) "the complete mechanics framework needed to extract toughness values for nanoscale films from membrane stretching experiments". Using the Begley-Mackin membrane deflection model [55] to extract both the effective modulus of the cracked multilayer, and electrically induced strain, they asserted that their proposed models were capable of predicting the coupled electromechanical response of previously described DEAs. They, also, indicated that electrode cracking should be promoted since it decreases the effective modulus of multilayer and improved charge distribution due to smaller crack openings.

Carpi and De Rossi [56], however, presented findings of their research activities in developing soft actuators made of silicon-based DEs with the potential applications as artificial muscles. In this regard, they introduced three applications; namely, eyeballs of an android robotic face, an anthropomorphic skeleton of upper limb, as well as a new robotic endoscope and investigated the actuation principle of these devices. They argued that despite such excellent features as sizable active strains and/or stresses in response to an electrical stimulus, low specific gravity, high grade of processability, down-scalability, and low costs, DEs required high driving electric fields (order of 10 - 100 $V/\mu m$) which prevented them from utilization in any intrabody applications. This problem could, however, be rectified by development of new improved materials and configurations which required lower driving voltage.

Seeking to establish a basis for the design of DEAs, Koo et al. [44] suggested an actuator controlled by an antagonistic drive mechanism, and examined the pre-strain effect on the actuation mechanism. Adopting Mooney-Rivlin theory describing the constitutive relation, they carried out the numerical analysis and verified their proposed design through an experiment.

Meanwhile, Mockensturm and Goulbourne [57] examined the dynamic behavior of one of the simplest possible DEs configurations i.e. an axisymmetric spherical inflated membrane subject to an electric field. Using the Mooney material model, the result of their work showed that the actuation of DEAs should be feasible with electric fields well below the breakdown field of the dielectric. Maintaining

the mechanical pressure constant during rapid inflation, they argued that despite the limited usefulness of such actuators due to their characteristics, they were still a good substitute to be exploited as an auxiliary device in the cardiovascular system.

In 2007, Patrick et al. [51] conducted a research aimed at examining the performance of planar DEAs under certain boundary conditions for quasi-static activation cycles. They modeled hyperelastic DEs using a three-dimensional coupled spring system which was equivalent to the constitutive model developed by Ogden. As for the electromechanical coupling applicable to their proposed DEAs, Patrick and co-workers introduced the equivalent electrode pressure in the thickness direction which covered two electromechanical effects; namely, (1) squeeze of the film by the electrodes due to the attraction of opposing charges in the thickness direction and (2) planar expansion of the film as a result of the repelling forces between equal charges on two electrodes. They further asserted that for DE two kinds of activation existed: activation with constant charge[2] and activation with constant voltage[3]; while the former led to only one equilibrium state, the latter predicted two equilibrium (stable and unstable) states. Introducing the critical voltage, they also suggested an electromechanical collapse should the voltage exceeded the critical value. And they finally concluded that the pre-stretching of DEs would lead to improved performance at lower initial activation field.

In the meantime, Plante and Dubowsky [58] highlighted the results of their study on the performance of DEAs in practical applications and proposed a design space considering pull-in failure, dielectric strength failure, viscoelasticity and current leakage as four major governing mechanisms. They developed an analytical model based on hyperelastic and Bergstrom-Boyce viscoelastic material models and verified the performance of DEAs over a range of actuation velocities. Discussing the possible applications of their design in robotics and mechantronics, Plante and Dubowsky compared such actuators with their electromagnetic counterparts.

Wissler and Mazza [1], however, investigated the electromechanical coupling in DEs both analytically and numerically in 2007. They conducted series of experiments on such actuators with different dielectric constants and prestretch ratio in order to validate their theoretical approach. The results of their work indicated a

[2]In this case the source is disconnected from the actuator after its initial electrical charging[51].
[3]In this case the source remains connected to the actuator during its active deformation [51].

consistency between the analytical and numerical assumptions and succeeded to verify the suggested equation of Pelrine [59] through theory and experiment.

Seeking to comprehend the major performance mechanisms of DEAs made of VHB 4905/4910 from 3M, Plante and Dubowsky [60] carried out an experimental investigation to portray the actuator performance in terms of force, power, current consumption, work output, and efficiency. They modeled the viscoelastic behavior of DEAs using a Mooney-Rivlin model in conjunction with Bergstrom-Boyce model. The result of their study revealed that viscoelasticity and current leakage were the restricting parameters for designing a DEA.

Motivated by the limited experimental efforts on the dynamic response analysis of DEAs, Fox and Goulbourne [49] conducted series of experiments in 2008. They performed their experiment on inflating planar DEs clamped-edge circular membranes. Owing to this fact, they centered their attention to enlarge these areas and experimentally quantify the large deformation dynamic behavior of DEAs membrane. To that end they prepared test specimen of their work by prestretching the commercially available VHB 4905 DE and fixing it in the test chamber as well as applying carbon grease as the compliant electrode on either sides of the membrane. Fox and Goulbourne later applied sinusoidal voltage (time-varying voltage) signals to a DEA and then varied harmonically the volume inside the test chamber using a piston pump (time-varying pressure loads). Using these experiments, one could achieve a pumping action by cycling the inflation and deflation of the membrane through constantly applying and removing the electric field. The results of their study indicated that the dynamic behavior of DEAs was the direct consequence of the classical dynamic response of membranes with all the attributes e.g. damping coefficients and mode-shapes. For DEAs all parts of the system, however, did not pass through the equilibrium simultaneously.

Fox and Goulbourne [61] highlighted the outcomes of a comprehensive experimental investigation intended to illustrate the dynamic deformation response of DE membranes. These membranes were fixed at their outer edge and subjected to a dynamic electric field and such variable systems parameters as chamber volume, initial flat state, and voltage offset. The numerical procedure of their work was based on the elastic membrane theory of Green and Adkins [62] and the electrostatic Maxwell stress effect. The numerical procedure was further calibrated with experimental data from inflation quasi-static tests of the DE membranes. It was evident from their work that electrical excitation of resonance phenomena could be

utilized in actuation applications, and the electric field could be used to transform a smooth monolithic structure into specific symmetry surface patterns which had a major advantage for adaptive structures. In addition they pointed out that the chamber volume was an important system parameter in dynamic DEs actuation.

More recently and motivated by the lack of published models for cone DEAs, Wang et al. [50] published a paper describing the finite element simulation, the manufacturing and the analysis of the working principle of such actuators. They applied Yeoh hyperelastic model for the finite element simulation used to predict the movement of the actuator. They, finally, pointed out that high active voltage was a major barrier in development of DEAs with real life applications.

3.3 Experiments

This section intends to provide a short overview of experiments with DEs. These experiments are aimed at providing electromechanical behavior of these materials [45]. In general experimental works with DEs fall into these two categories [45]: (1) quasi-static experiments and (2) dynamics experiments.

Quasi-static experiments consist of *uniaxial compression tests*, *tensile tests*, and *biaxially pre-strained circular actuator experiments* [48, 63]. The first two tests are served to provide such material parameters as compressive moduli and tensile moduli, while the biaxial pre-strained test are usually performed after the first two tests is used to mimic the electrical actuation conditions between compliant electrodes [63].

Dynamic experiments, on the other hand, are exploited to study the dynamic response of DEs. They comprise of *dynamic mechanical loading experiments* and *dynamic electrical loading experiments*. While the former is carried out using a dynamic pressure input, the latter measures the dynamic electrical loading response due to a dynamic voltage input [45]. For an extensive coverage of the experimental procedures and set-up associated with DEs the interested readers are referred to Ref. [45]

3.4 Applications

To wrap up this chapter some major applications of DEs as appeared in [64] are presented. One can find DEs' presence in such application areas as (1) biomedicine with haptic and micro-scale applications, (2) robotics with biorobotic applications and (3) industry with commercial applications.

Examples of biomedical applications include orthotics and prosthetics, force feedback devices, microactuators, micro-optics, and a new Braille displaye system design [64]. Biommimetic robots, micro-annelid-like robot actuated by artificial muscles, binary actuators, robotic arm, on the other hand, can be mentioned as some of the applications of DEs in Robotics. And finally loudspeakers are a good example of DEs commercial application.

Chapter 4

Modeling of Dielectric Elastomers

4.1 Introduction to Nonlinear Analysis

In the following a rather brief introduction to nonlinear analysis will be presented. The facts and theories throughout this chapter are adopted from Ref. [65–70].

Most problems in solid mechanics are nonlinear in nature. Linear assumptions would only result in approximate solutions which, often, do not represent the actual behavior of the system. In order to study the nonlinear behavior of the mechanical systems it is necessary to first classify different sources of nonlinearities. In this regard geometrical nonlinearities, material nonlinearities and nonlinear boundary conditions comprise the sources of nonlinearities.

Geometrical nonlinearities are accounted for in situations where a solid reaches a state for which undeformed and deformed shapes are substantially different [65]. Typical examples of geometrical nonlinearities are structural instability analyses, forming processes, crash and impact problems.

Material nonlinearities, however, stem themselves from the nonlinear stress-strain behavior in the constitutive model of the material [66]. Relevant nonlinear material models include nonlinear (hyper-) elasticity, plasticity, viscoelasticity, creep and damage.

Nonlinear boundary conditions, on the other hand, are the result of large deformation [66]. Examples of such nonlinearities are pressure loadings that remain normal to the deformed body and also the case where the deformed boundary interacts

with another body, i.e. contact problems [65]. In the current work, however, the first two forms of nonlinearities i.e. geometrical and material nonlinearities are of primary concerns.

In the context of the finite element method, the governing equations describing such nonlinear behaviors are generally expressed in a weak integral form using for example the principle of virtual work. Manipulating these integral equations yield a finite set of nonlinear algebraic equations which are usually solved utilizing the Newton-Raphson iterative schemes [66].

In the next sections, some pertinent aspects of nonlinear continuum mechanics will be reviewed followed by the formulation of the constitutive equations and finite element implementation of the presented constitutive model for dielectric elastomers.

4.2 Nonlinear Continuum Mechanics

4.2.1 Continuum Body

A *continuum body* is a macroscopic system given by infinite number of particles defining for instance a solid, a liquid, a gas or an intermediate state. It is assumed that there is no discontinuity between the particles and the mathematical functions describing the motion and properties of the continuum body are continuous functions.

The concept of *configuration* is the necessary tool to derive further equations describing kinematics and motion of a continuum body. At each instance of time t, a continuum body occupies a different region in space referring here to as Ω_t which by reference to a suitable set of coordinate system is said to specify the configuration of the continuum body at that instance of time. The configuration Ω_0 at $t = 0$ is commonly referred to as reference or material configuration, while any other configuration at time $t > 0$ is called current, spatial or deformed configuration.

Current and reference configurations can be converted to each other through the so-called the motion mapping and the inverse motion mapping. Denoting $\mathbf{X}$ as the position vector of a particle $\mathcal{P}$ in reference configuration and $\mathbf{x}$ as the position

vector of a particle $\mathcal{P}$ in current configuration, the motion mapping is defined as:

$$\mathbf{x} = \varphi(\mathbf{X}, t) \tag{4.1}$$

Conversely, the inverse motion mapping is defined as:

$$\mathbf{X} = \varphi^{-1}(\mathbf{x}, t) \tag{4.2}$$

It is assumed that such mappings are one-to-one and continuous, with continuous partial derivatives to whatever order which is required [67]. The description of motion or deformation expressed by Eq. (4.1) is known as *material* or *Lagrangian* description of motion, whereas the description of motion expressed by Eq. (4.2) is commonly referred to as *spatial* or *Eulerian* description of motion [67].

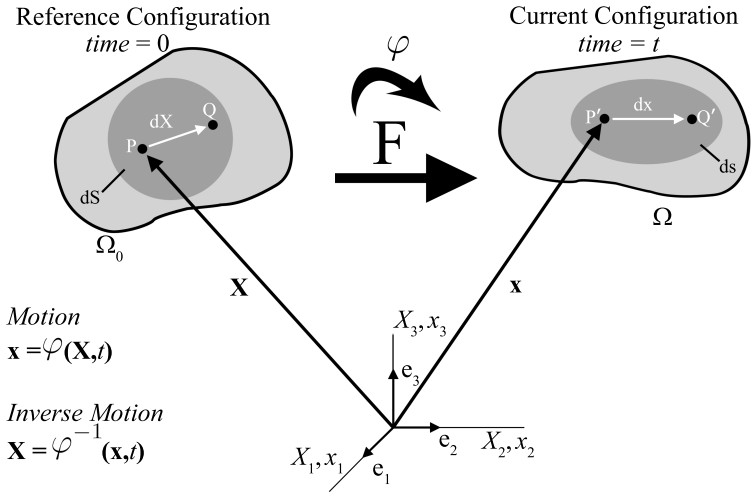

FIGURE 4.1: Motion of a continuum body

4.2.2 Deformation Gradient Tensors

As the fundamental kinematic variable in solid mechanics, material deformation gradient is in general a nonsymmetric tensor defined as the partial differentiation of Eq. (4.1) with respect to $\mathbf{X}$. It maps the material tangent vector $d\mathbf{X}$ onto the spatial tangent vector $d\mathbf{x}$:

$$d\mathbf{x} = \mathbf{F}.d\mathbf{X} \qquad or \qquad \mathbf{F} = \frac{d\mathbf{x}}{d\mathbf{X}} = GRAD\mathbf{x} \tag{4.3}$$

The inverse deformation gradient, on the other hand, is defined as the partial differentiation of Eq. (4.2) with respect to $\mathbf{x}$. It maps the spatial tangent vector $d\mathbf{x}$ onto the material tangent vector $d\mathbf{X}$:

$$d\mathbf{X} = \mathbf{F}^{-1}.d\mathbf{x} \qquad or \qquad \mathbf{F}^{-1} = \frac{d\mathbf{X}}{d\mathbf{x}} = grad\mathbf{X} \tag{4.4}$$

4.2.3 Strain Tensors

In nonlinear continuum mechanics such strain tensors as Green-Lagrange and Euler-Almansi strain tensors are introduced in order to establish a relation between the undeformed (reference) and deformed (current) configurations.

Green-Lagrange strain tensor, $\mathbf{E}$, is a material symmetric second order tensor which is deduced when the deformation is measured as the difference between the square of the spatial length, dl, and the material length, dL. Expressing the square of the spatial length as $dl^2 = d\mathbf{x}.d\mathbf{x}$ and the square of the material length as $dL^2 = d\mathbf{X}.d\mathbf{X}$, one has:

$$\begin{aligned} dl^2 - dL^2 &= d\mathbf{x}.d\mathbf{x} - d\mathbf{X}.d\mathbf{X} \\ &= \mathbf{F}d\mathbf{X}.\mathbf{F}d\mathbf{X} - d\mathbf{X}.d\mathbf{X} \\ &= d\mathbf{X}\mathbf{F}^T\mathbf{F}d\mathbf{X} - d\mathbf{X}.d\mathbf{X} \\ &= d\mathbf{X}.(\mathbf{F}^T\mathbf{F} - \mathbf{I})d\mathbf{X} \\ &= 2d\mathbf{X}.\mathbf{E}.d\mathbf{X} \end{aligned}$$

Green-Lagrange strain tensor, $\mathbf{E}$, is then defined as:

$$\mathbf{E} := \frac{1}{2}(\mathbf{F}^T\mathbf{F} - \mathbf{I}) \tag{4.5}$$

where, $\mathbf{I}$ is the second-order identity tensor:

$$\mathbf{I} = \begin{bmatrix} 1 & 0 & 0 \\ 0 & 1 & 0 \\ 0 & 0 & 1 \end{bmatrix} \tag{4.6}$$

Euler-Almansi strain tensor, $\mathbf{e}$, on the other hand, is a spatial symmetric second order tensor which is also derived when the deformation is measured as the difference between the square of the spatial length, dl, and the material length,

dL. Expressing the square of the spatial length as $dl^2 = d\mathbf{x}.d\mathbf{x}$ and the square of the material length as $dL^2 = d\mathbf{X}.d\mathbf{X}$, one has:

$$\begin{aligned} dl^2 - dL^2 &= d\mathbf{x}.d\mathbf{x} - d\mathbf{X}.d\mathbf{X} \\ &= d\mathbf{x}.d\mathbf{x} - \mathbf{F}^{-1}d\mathbf{x}\mathbf{F}^{-1}d\mathbf{x} \\ &= d\mathbf{x}.d\mathbf{x} - d\mathbf{x}\mathbf{F}^{-T}\mathbf{F}^{-1}d\mathbf{x} \\ &= d\mathbf{x}.(\mathbf{I} - \mathbf{F}^{-T}\mathbf{F}^{-1})d\mathbf{x} \\ &= 2d\mathbf{x}.\mathbf{e}.d\mathbf{x} \end{aligned}$$

Euler-Almansi strain tensor, $\mathbf{e}$, is then defined as:

$$\mathbf{e} := \frac{1}{2}(\mathbf{I} - \mathbf{F}^{-T}\mathbf{F}^{-1}) \tag{4.7}$$

4.2.4 The Concept of Stress

Prior to the introduction of the concept of stress in continuum mechanics it is necessary to have a basic understanding of some other preliminary concepts. First, forces acting on a continuum body are discussed. In the context of nonlinear continuum mechanics, two types of forces; namely, body forces and surface forces, are usually considered. Body forces also known as internal forces act within a continuum body. Typical examples of such forces are the gravity forces, electromagnetic forces, etc. On the contrary, surface forces act on outer boundary of a continuum body. Contact forces between bodies or applied forces on the surface of a body are some examples of surface forces.

Another prerequisite to the concept of stress is the idea of traction vector or stress vector. Considering $d\mathbf{f}$ as the resultant current infinitesimal force acting on the surface element, ds, in the current configuration (Fig. 4.2), Cauchy or true traction vector, $\mathbf{t}$, is then mathematically defined as:

$$\mathbf{t} = \frac{d\mathbf{f}}{ds} \tag{4.8}$$

The first Piola-Kirchhoff or nominal traction vector, $\mathbf{T}$, on the other hand, is defined as:

$$\mathbf{T} = \frac{d\mathbf{f}}{dS} \tag{4.9}$$

Where, dS is the surface element in the reference configuration.

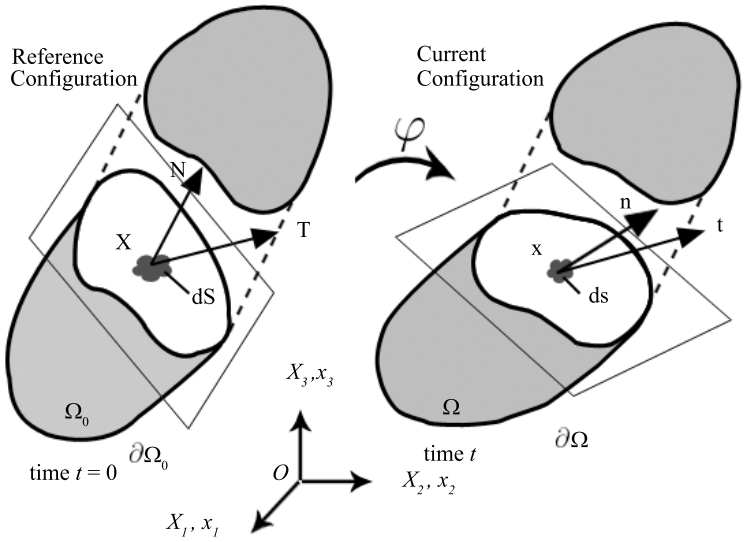

FIGURE 4.2: Traction vector

By the introduction of the abovementioned preliminaries, it is now possible to present the definition of the stress tensors in a continuum body. By virtue of the Cauchy's stress principle, one can associate the true traction vector, $\mathbf{t}$, at an arbitrary point inside the continuum body to the unit normal vector, $\mathbf{n}$, in the current configuration as illustrated in Fig. 4.2. This leads to the definition of the Cauchy or true stress tensor, $\boldsymbol{\sigma}$, as:

$$\mathbf{t} = \boldsymbol{\sigma}\mathbf{n} \tag{4.10}$$

which is a second order symmetric tensor ($\boldsymbol{\sigma} = \boldsymbol{\sigma}^T$). Using a matrix notation, the cartesian components of the Cauchy or true stress tensor, then, are:

$$\boldsymbol{\sigma} = \begin{bmatrix} \sigma_{11} & \sigma_{12} & \sigma_{13} \\ \sigma_{12} & \sigma_{22} & \sigma_{23} \\ \sigma_{13} & \sigma_{23} & \sigma_{33} \end{bmatrix}$$

The components of the Cauchy stress tensor have also been depicted in Fig. 4.3

Conversely, the first Piola-Kirchhoff or nominal stress tensor, $\mathbf{P}$, is defined as:

$$\mathbf{T} = \mathbf{P}\mathbf{N} \tag{4.11}$$

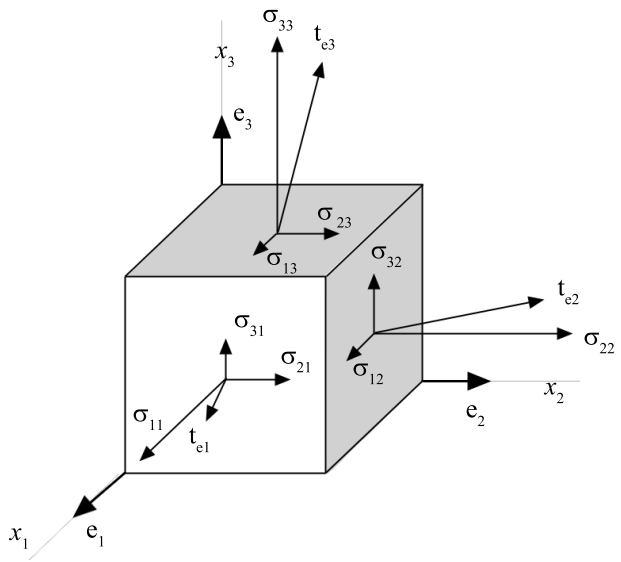

FIGURE 4.3: Cauchy's stress tensor components

Where **N** is the unit normal vector in the reference configuration. These two stress tensors are related to each other through the following expression:

$$\boldsymbol{\sigma} = \frac{1}{det\mathbf{F}}\mathbf{P}\mathbf{F}^T \tag{4.12}$$

Other stress tensors which are worth mentioning here are the second Piola-Kirchhoff and Kirchhoff stress tensors. The second Piola-Kirchhoff stress tensor, **S**, is related to the Cauchy stress tensor as:

$$\mathbf{S} = det\mathbf{F}\ \mathbf{F}^{-1}\boldsymbol{\sigma}\ \mathbf{F}^{-T} \tag{4.13}$$

While, Kirchhoff stress tensor, $\boldsymbol{\tau}$, is related to Cauchy stress tensor such that:

$$\boldsymbol{\tau} = det\mathbf{F}\ \boldsymbol{\sigma} \tag{4.14}$$

It is also worth mentioning that for each one of the abovementioned stress tensors there is an energetically conjugate strain tensor provided that the (virtual) energy is not affected by the choice of a certain pair of stresses and strains. In this regard, second Piola-Kirchhoff stresses and Green-Lagrange strains are energetically conjugate. Other energetically conjugate pairs of stresses and strains are: deformation gradient and first Piola-Kirchhoff stresses, Euler-Almansi strains and Cauchy stresses.

4.3 Infinitesimal Strain Theory

4.3.1 General Overview

Since the analyses associated with the current study are mostly based on the infinitesimal (small) strain theory, it is essential to introduce the basic assumptions used therein. These include:

1. No distinction between current (deformed) configuration and reference configuration is considered:

$$\Omega_0 \cong \Omega \tag{4.15}$$

2. No distinction between material coordinates (at the reference configuration) and spatial coordinates (at the current deformed configuration) is considered:

$$\mathbf{x} = \mathbf{X} \tag{4.16}$$

3. No distinction between material and spatial descriptions is considered.

4. No difference between material and spatial differential operators (e.g. gradient and divergence) is considered.

One of the direct consequences of the infinitesimal strain theory is that all the strain tensors are considered the same, given by:

$$\boldsymbol{\varepsilon} := sym[\nabla \mathbf{u}] = \frac{1}{2}[\nabla \mathbf{u} + \nabla \mathbf{u}^T] \tag{4.17}$$

where $\mathbf{u}$ is the displacement tensor.

4.3.2 Voigt-Notation

Taking advantage of the symmetric properties of the stress and strain tensors[1], it is always more practical to exploit the so-called Voigt-Notation instead of the

[1]The symmetric properties of stresses come from the balance of angular momentum while the symmetric properties of strains is the consequence of infinitesimal strain assumption.

full tensorial notation especially in nonlinear finite element analysis due to less computer storage requirement.

In small strain theory, the stress tensor and the strain tensor can be related by a linear relation, such that:

$$\sigma_{ij} = \sum_{k,l=1}^{3} \mathbb{C}_{ijkl}\varepsilon_{ij} \tag{4.18}$$

σ_{ij} and ε_{ij} are the components of the stress tensor and the strain tensor, respectively. The numbers $\mathbb{C}_{ijkl}$ are called the elastic coefficients. There are 81 of these components. Together, they form the elasticity tensor, $\mathbb{C}$. Due to the symmetric properties of the stress tensor and the strain tensor i.e. $\sigma_{ij} = \sigma_{ji}$ and $\varepsilon_{ij} = \varepsilon_{ji}$, $\mathbb{C}_{ijkl} = \mathbb{C}_{ijlk}$ and $\mathbb{C}_{ijkl} = \mathbb{C}_{jikl}$ (these relations are called minor-symmetries). Hence, instead of 81 independent coefficients, $\mathbb{C}$ will have only 36. Therefore, one has:

$$\sigma_{ij} = \mathbb{C}_{ij11}\varepsilon_{11} + \mathbb{C}_{ij22}\varepsilon_{22} + \mathbb{C}_{ij33}\varepsilon_{33} + \mathbb{C}_{ij23}(2\varepsilon_{23}) + \mathbb{C}_{ij13}(2\varepsilon_{13}) + \mathbb{C}_{ij12}(2\varepsilon_{12}) \tag{4.19}$$

In this regard, the stress tensor, $\boldsymbol{\sigma}$, can now be re-written in Voigt-Notation as:

$$\boldsymbol{\sigma} = \begin{bmatrix} \sigma_{11} & \sigma_{12} & \sigma_{13} \\ \sigma_{12} & \sigma_{22} & \sigma_{23} \\ \sigma_{13} & \sigma_{23} & \sigma_{33} \end{bmatrix} \quad \longrightarrow \quad \boldsymbol{\sigma} = \begin{pmatrix} \sigma_{11} \\ \sigma_{22} \\ \sigma_{33} \\ \sigma_{23} \\ \sigma_{13} \\ \sigma_{12} \end{pmatrix}$$

Accordingly, one can write the strain tensor in Voigt-Notation as:

$$\boldsymbol{\varepsilon} = \begin{bmatrix} \varepsilon_{11} & \varepsilon_{12} & \varepsilon_{13} \\ \varepsilon_{12} & \varepsilon_{22} & \varepsilon_{23} \\ \varepsilon_{13} & \varepsilon_{23} & \varepsilon_{33} \end{bmatrix} \quad \longrightarrow \quad \boldsymbol{\varepsilon} = \begin{pmatrix} \varepsilon_{11} \\ \varepsilon_{22} \\ \varepsilon_{33} \\ 2\varepsilon_{23} \\ 2\varepsilon_{13} \\ 2\varepsilon_{12} \end{pmatrix}$$

In this work, Voigt-Notation will be used.

4.3.3 Spherical and Deviatoric Tensors

In nonlinear continuum mechanics, a strain tensor can be viewed as an additive split of the so-called volumetric and deviatoric parts. Volumetric strain, e, also known as spherical strain is a scalar quantity which describes the dilatation or the relative variation of the volume in the continuum body. It is mathematically defined as the trace of the strain tensor:

$$e := tr[\boldsymbol{\varepsilon}] = \varepsilon_{11} + \varepsilon_{22} + \varepsilon_{33} \tag{4.20}$$

The deviatoric part of the strain, $\boldsymbol{\varepsilon}'$, also known as isochoric strain is the volume preserving strain and is defined as:

$$\boldsymbol{\varepsilon}' = \boldsymbol{\varepsilon} \; - \; \frac{1}{3} tr[\boldsymbol{\varepsilon}]\mathbf{I} \tag{4.21}$$

where, $\mathbf{I}$, is the second-order identity tensor.

Accordingly, the stress tensor can be viewed as an additive split of the spherical part and deviatoric part such that:

$$\boldsymbol{\sigma}_{esp} = \frac{1}{3} tr[\boldsymbol{\sigma}]\mathbf{I} \tag{4.22}$$

is the spherical part of the stress, and

$$\boldsymbol{\sigma}' = \boldsymbol{\sigma} \; - \; \frac{1}{3} tr[\boldsymbol{\sigma}]\mathbf{I} \tag{4.23}$$

is the deviatoric part of the stress.

4.4 Balance Laws

Balance laws as well as some restriction principles, e.g. second law of thermodynamics are required to derive the governing equations of a continuum body. The resulting system of equations, however, can only be solved in conjunction with kinematic relation, as explained in the previous sections, and constitutive equations.

Balance laws can mathematically be expressed in either the integral (global) form or the strong (local) form. Each one of these representations can also be cast either in reference (material) or current (spatial) configurations. These laws include, *Conservation of Mass*, *Balance of Linear Momentum*, *Balance of Angular Momentum*, *Energy Balance* along with the *Second Law of Thermodynamics* as the restriction.

Conservation of Mass states that during a motion there are neither mass sources nor mass sinks and the mass, m, of a continuum body is conserved. The global and local spatial forms of conservation of mass can, therefore, be expressed as Eq. (4.24) and Eq. (4.25), respectively:

$$\frac{d}{dt}\int_{\Omega}\rho\, dv = 0 \tag{4.24}$$

$$\frac{\partial\rho}{\partial t} + \rho(div\mathbf{v}) = 0 \tag{4.25}$$

Where, ρ is the density, v is the volume of the continuum body, Ω, and $\mathbf{v}$ is the velocity.

Balance of Linear Momentum states that the time-variation of the linear momentum of a material volume is equal to the resultant force acting on the material volume. The global and local spatial forms of balance of linear momentum are presented as, Eq. (4.26) and Eq. (4.27), respectively.

$$\frac{d}{dt}(\mathbf{M}_{\mathrm{L}}) = \mathcal{F} \tag{4.26}$$

$$\rho\frac{\partial\mathbf{v}}{\partial t} = div[\boldsymbol{\sigma}] + \rho\mathbf{b} \tag{4.27}$$

where $\mathcal{F} = \int_{\Omega}\rho\mathbf{b}\, d\Omega + \int_{\partial\Omega}\mathbf{t}\, d\partial\Omega$. Here $\mathbf{b}$ represents the body forces, $\mathbf{t}$ is the traction vector, and $\partial\Omega$ is the surface area of the continuum body.

Balance of Angular Momentum, on the other hand, states that the time-variation of the angular momentum of a material volume with respect to a fixed point, $\mathbf{M}_{\mathrm{O}}$, is equal to the resultant moment with respect to this fixed point, $\mathbf{M}$. The global and local spatial forms of balance of angular momentum are presented

as, Eq. (4.28) and Eq. (4.29), respectively.

$$\frac{d}{dt}(\mathbf{M}_{\mathrm{O}}) = \mathbf{M} \quad or \quad \frac{d}{dt}\int_{\Omega} \mathbf{r} \times \rho \mathbf{v}\, d\Omega = \int_{\Omega} \mathbf{r} \times \rho \mathbf{b}\, d\Omega + \int_{\partial\Omega} \mathbf{r} \times \mathbf{t}\, d\partial\Omega \tag{4.28}$$

$$\boldsymbol{\sigma} = \boldsymbol{\sigma}^{\boldsymbol{T}} \tag{4.29}$$

where, $\mathbf{r} = \mathbf{x} - \mathbf{x}_0$, is the distance from point O. The Equation (4.29) is interpreted as the symmetry of the Cauchy stress tensor.

Balance of Energy states that the material time derivative of the total energy of the system is equal to the *External Mechanical Power* and *External Thermal Power*. Defining external mechanical power as:

$$P_{ext} := \int_{\Omega} \rho \mathbf{b} \cdot \mathbf{v}\, d\Omega + \int_{\partial\Omega} \mathbf{t} \cdot \mathbf{v}\, d\partial\Omega \tag{4.30}$$

and external thermal power as:

$$Q_{ext} := \int_{\Omega} \rho \mathbf{r}\, d\Omega \; - \; \int_{\partial\Omega} \mathbf{q} \cdot \mathbf{n}\, d\partial\Omega \tag{4.31}$$

Balance of energy is mathematically expressed as:

$$\frac{d}{dt}(E + K) = P_{ext} + Q_{ext} \tag{4.32}$$

where E is the internal energy, K is the kinetic energy, and $\mathbf{q}$ is the spatial heat flux per unit of spatial surface area, $\partial\Omega$, in the current configuration.

The First Law of Thermodynamics states that the material time derivative of the total energy is equal to the material time derivatives of the kinetic and internal energy. This can be mathematically presented as:

$$\rho \dot{e} = \boldsymbol{\sigma} : \dot{\boldsymbol{\varepsilon}} + \rho r \; - \; div\mathbf{q} \tag{4.33}$$

where e is the internal energy per unit mass and r is the internal heat source rate per unit of mass.

The Second Law of Thermodynamics states that the material time derivative of the entropy, H, must always be greater or equal to the rate of the entropy input into the system. The rate of the entropy , $\dot{\eta}$, is defined as the rate of the total

amount of heat per unit of temperature input to the system (both due to internal sources across the boundaries). Assuming ρ to be constant, the second law of thermodynamics is now expressed as:

$$\frac{d}{dt}H = \frac{d}{dt}\int_{\Omega}\rho\eta\, d\Omega = \int_{\Omega}\rho\dot{\eta}\, d\Omega \geq \int_{\Omega}\rho\frac{r}{\theta}\, d\Omega \; - \; \int_{\partial\Omega}\frac{\mathbf{q}}{\theta}\cdot\mathbf{n}\, d\partial\Omega \tag{4.34}$$

which when expressed in local form, is known as "Clausius-Duhem inequality":

$$\rho\dot{\eta} \geq \rho\frac{r}{\theta} \; - \; div\frac{\mathbf{q}}{\theta} = \rho\frac{r}{\theta} \; - \; \frac{1}{\theta}div\mathbf{q} + \frac{1}{\theta^2}\mathbf{q}\cdot grad\theta \tag{4.35}$$

where, η is entropy per unit of mass or specific entropy.

The fundamental governing equations arising from the aforementioned laws and principles yield a system of equations which can only be solved with the help of constitutive equations and suitable boundary conditions. Such equations are also known as "Initial Boundary Value Problem (IBVP)".

4.5 Constitutive Equations

4.5.1 General Overview

In this section the derivation of the constitutive equations based on the assumption of infinitesimal strain is presented. These constitutive equations are formulated such that they satisfy *the second axiom of irreversibility* for all admissible (general) process. "Good" constitutive equations satisfy the second axiom, which is expressed as:

$$\begin{aligned}\rho\mathcal{D}_{local} &:= \boldsymbol{\sigma} : \dot{\boldsymbol{\varepsilon}} - \rho\eta\dot{\theta} - \dot{\Psi} \geq 0\\ \rho\mathcal{D}_{con} &:= -\frac{1}{\theta}\mathbf{q}\cdot\nabla\theta\end{aligned} \tag{4.36}$$

These two inequalities are known as the "Clausius-Planck inequality" and the "Fourier inequality", respectively. Here, $\Psi := e - \theta\eta$ is the Helmholtz free energy per unit of mass or specific free energy, $\mathcal{D}_{local}$ is the rate of internal dissipation per unit of spatial volume, and $\mathcal{D}_{con}$ is the rate of dissipation by heat conduction per unit of spatial volume.

The formulation of the constitutive equations, here, follows the *general internal variable formulation*, where a generalized vector $\mathcal{I} \in \mathcal{R}^n$ of internal variable is, first, introduced (e.g. viscous strain, $\boldsymbol{\varepsilon}_s$, plastic strain, $\boldsymbol{\varepsilon}^p$, $\cdots$). Two fundamental constitutive functions are, further, exploited, i.e. *Energy Storage* function, Ψ, and *Dissipation* function, Φ. The former governs the storage mechanics ("spring") whereas the latter governs the dissipative mechanism. This is illustrated in Fig. 4.4.

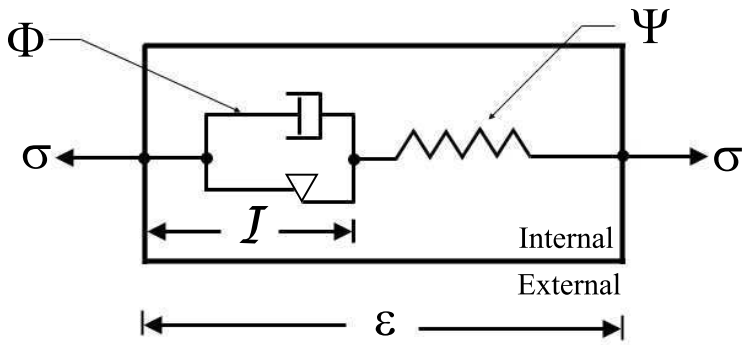

FIGURE 4.4: Material box

These two functions govern a broad class of inelastic material models and using the so-called "Coleman's Exploitation Method", one can derive the constitutive equations. This is demonstrated as follows:

assuming,

$$\Psi = \hat{\Psi}(\boldsymbol{\varepsilon}, \theta, \mathcal{I}) \tag{4.37}$$

and

$$\Phi = \hat{\Phi}(\mathcal{F}) \tag{4.38}$$

the Clausius–Planck ineqaulity can be re-written as:

$$\rho \mathcal{D}_{local} = [\boldsymbol{\sigma} - \rho \partial_{\boldsymbol{\varepsilon}} \hat{\Psi}] : \dot{\boldsymbol{\varepsilon}} - \rho[\eta + \partial_{\boldsymbol{\sigma}} \hat{\Psi}] \cdot \dot{\theta} - \rho \partial_{\mathcal{I}} \hat{\Psi} \cdot \dot{\mathcal{I}} \geq 0 \tag{4.39}$$

This procedure will ensure the thermodynamic consistency of the material model.

Using the Coleman's Exploitation Method yields the following constitutive equations for stresses, entropy and internal forces:

$$\boldsymbol{\sigma} = \rho \partial_{\boldsymbol{\varepsilon}} \hat{\Psi}(\boldsymbol{\varepsilon}, \theta, \mathcal{I}) \tag{4.40}$$

$$\eta = -\partial_{\theta} \hat{\Psi}(\boldsymbol{\varepsilon}, \theta, \mathcal{I}) \tag{4.41}$$

$$\mathcal{F} = \partial_{\mathcal{I}} \hat{\Psi}(\boldsymbol{\varepsilon}, \theta, \mathcal{I}) \tag{4.42}$$

4.5.2 3D Formulation of the Viscoelastic Constitutive Model

A three dimensional formulation of the viscoelastic constitutive model presented here is based on the Maxwell material (Fig. 4.5) which is the most general *linear* viscoelastic model. Assuming a volumetric-isochoric split of strain, the two fundamental functions for the free energy, Ψ, and dissipation functional, Φ, are expressed as:

$$\Psi(\boldsymbol{\varepsilon}, \boldsymbol{\alpha}_1, \cdots, \boldsymbol{\alpha}_n) = \frac{1}{2}\kappa e^2 + \mu_0 \|\boldsymbol{\varepsilon}'\|^2 + \sum_{i=1}^{n} \mu_i \|\boldsymbol{\varepsilon}' - \boldsymbol{\alpha}_i\|^2 \tag{4.43}$$

$$\Phi(\boldsymbol{\beta}_1, \cdots, \boldsymbol{\beta}_n) = \sum_{i=1}^{n} \frac{1}{2} \frac{1}{\eta_i} \|\boldsymbol{\beta}_i\|^2 \tag{4.44}$$

where, $\boldsymbol{\alpha}_i$, are the tensors of the internal variables, $\boldsymbol{\beta}_i$, are the tensors of the internal forces, κ is the bulk modulus, $\eta_i = \mu_i \tau_i$ is the viscosity of the dashpots, τ_i is the relaxation time, μ_i is the shear modulus of the springs in the Maxwell arm, μ_0 is the ground shear modulus, e is the trace of the strain tensor, and $\boldsymbol{\varepsilon}'$ is the deviatoric strain.

Using the Coleman's exploitation method, i.e. :

$$\boldsymbol{\sigma} = \partial_{\boldsymbol{\varepsilon}} \Psi \quad ; \quad \boldsymbol{\beta}_i = -\partial_{\boldsymbol{\alpha}_i} \Psi \quad ; \quad \dot{\boldsymbol{\alpha}}_i = \partial_{\boldsymbol{\beta}_i} \Phi \tag{4.45}$$

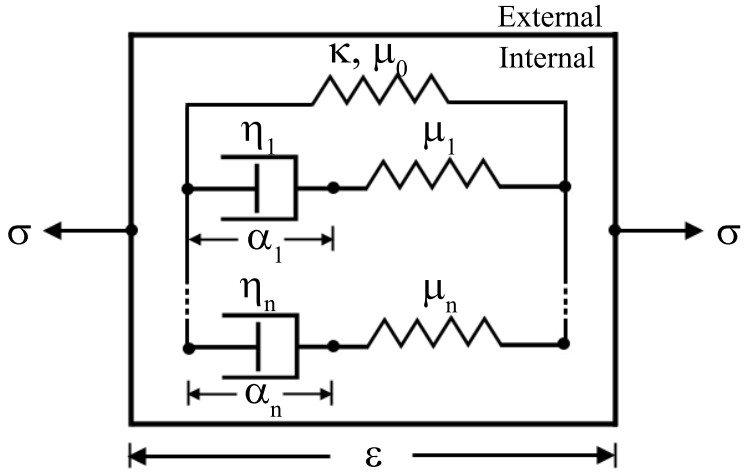

FIGURE 4.5: Generalized Maxwell model

one ends up with the following three representations for viscoelasticity constitutive equations.

$$\textbf{Representation A}: \begin{cases} \boldsymbol{\sigma} & = (\kappa e)\mathbf{I} + [2\mu_0\boldsymbol{\varepsilon}' + \sum_{i=1}^{n} 2\mu_i(\boldsymbol{\varepsilon}' - \boldsymbol{\alpha}_i)] : \mathbb{P} \\ \boldsymbol{\beta}_i & = 2\mu_i(\boldsymbol{\varepsilon}' - \boldsymbol{\alpha}_i) \\ \dot{\boldsymbol{\alpha}}_i & = \frac{1}{\eta_i}\boldsymbol{\beta}_i \end{cases} \tag{4.46}$$

$$\textbf{Representation B}: \begin{cases} \boldsymbol{\sigma} & = (\kappa e)\mathbf{I} + 2\mu_0\boldsymbol{\varepsilon}' + \sum_{i=1}^{n} \boldsymbol{\beta}_i \\ \\ \dot{\boldsymbol{\beta}}_i + \frac{1}{\tau_i}\boldsymbol{\beta}_i & = 2\mu_i\dot{\boldsymbol{\varepsilon}}' \end{cases} \tag{4.47}$$

$$\textbf{Representation C}: \begin{cases} \boldsymbol{\sigma} & = (\kappa e)\mathbf{I} + \int_0^t 2\hat{\mu}(t-s)\dot{\boldsymbol{\varepsilon}}'(s)\, ds \\ \\ \hat{\mu}(t) & = \mu_0 + \sum_{i=1}^{n} \mu_i exp(\frac{-t}{\tau_i}) \end{cases} \tag{4.48}$$

Some remarks should be added at this point:

- Representation B is obtained by elimination of the internal variables, $\boldsymbol{\alpha}_i$.
- Integration of the evolution equation, $\dot{\boldsymbol{\alpha}}_i = \frac{1}{\eta_i}\boldsymbol{\beta}_i$ results in representation C. This representation which is the most compact representation is known as *the convolution representation of viscoelasticity*. The other two are the differential representations of the viscoelasticity.

- Notation $\|\boldsymbol{\varepsilon}'\|^2 = \boldsymbol{\varepsilon}' : \boldsymbol{\varepsilon}'$ is the norm of the second order deviatoric strain tensor, $\boldsymbol{\varepsilon}'$
- $\hat{\mu}(t) = \mu_0 + \sum_{i=1}^{n} \mu_i exp(\frac{-t}{\tau_i})$ is the shear modulus relaxation function
- $\mathbb{P} := \mathbb{I} - \frac{1}{3}\mathbf{I} \otimes \mathbf{I}$ is the fourth order deviatoric projection tensor and is defined as:

$$\mathbb{P} = \begin{bmatrix} \frac{2}{3} & -\frac{1}{3} & -\frac{1}{3} & 0 & 0 & 0 \\ -\frac{1}{3} & \frac{2}{3} & -\frac{1}{3} & 0 & 0 & 0 \\ -\frac{1}{3} & -\frac{1}{3} & \frac{2}{3} & 0 & 0 & 0 \\ 0 & 0 & 0 & \frac{1}{2} & 0 & 0 \\ 0 & 0 & 0 & 0 & \frac{1}{2} & 0 \\ 0 & 0 & 0 & 0 & 0 & \frac{1}{2} \end{bmatrix}$$

where, $\mathbb{I}$ is the fourth-order identity tensor and is defined as:

$$\mathbb{I} = \begin{bmatrix} 1 & 0 & 0 & 0 & 0 & 0 \\ 0 & 1 & 0 & 0 & 0 & 0 \\ 0 & 0 & 1 & 0 & 0 & 0 \\ 0 & 0 & 0 & 0 & 0 & 0 \\ 0 & 0 & 0 & 0 & 0 & 0 \\ 0 & 0 & 0 & 0 & 0 & 0 \end{bmatrix}$$

4.5.3 Constitutive Model for Dielectric Elastomers

As mentioned in Sec. 3.2, the main challenge in developing the constitutive equations for DEs is the treatment of the electromechanical coupling in DEs placed in an electric field. According to Goulbourne et al. [6] the state of stress at a point in the deformed (activated) medium is determined by (1) the local elastic state of the medium and (2) the electrostatic effect due to the presence of an electric field. The latter effect renders itself as the so-called "Maxwell stress", $\boldsymbol{\sigma}_M$, which is defined as:

$$\boldsymbol{\sigma}_M = \varepsilon_0 \varepsilon_r \mathbf{E} \otimes \mathbf{E} - \varepsilon_0 \varepsilon_r \frac{\tilde{E}^2}{2} \tag{4.49}$$

where, $\varepsilon_0 = 8.854 \ . \ 10^{-12} \ \frac{\text{As}}{\text{Vm}}^2$ is the free-space permittivity, ε_r is the dielectric constant of the material, $\mathbf{E}$ is tensor of electric field and $\tilde{E}$ is the amount of electric

[2] Amper second per Volt meter

field in the prefered direcetion and is given by:

$$\tilde{E} = \frac{U}{z} \tag{4.50}$$

where U is the voltage and z refers to the thickness in the prefered direction.

Having said that, the Cauchy (true) stress tensor can now be defined as the augmentation of elastic tensor, $\boldsymbol{\sigma}_E$, with the Maxwell stress, $\boldsymbol{\sigma}_M$, such that [6]:

$$\boldsymbol{\sigma} = \boldsymbol{\sigma}_E + \boldsymbol{\sigma}_M \tag{4.51}$$

It is evident from the aforementioned relation that upon removal of the electric field the Cauchy stress tensor renders itself as the elastic tensor. For a uniform electric field applied in the thickness direction, the stress components of the Maxwell stress tensor take the form [61]:

$$(\boldsymbol{\sigma_M})_{ij} = \begin{cases} \mp \dfrac{\varepsilon_0 \varepsilon_r U^2}{2\left(\lambda_t z_0\right)^2} & i = j \\ 0 & i \neq j \end{cases} \tag{4.52}$$

where, λ_t is the stretch in the thickness direction defined as the ratio between the thickness in the current configuration and the thickness in the reference configuration. z_0 is the original DE thickness and $\lambda_t z_0$ corresponds to instantaneous material thickness. The principal stresses now become:

$$\begin{aligned} \sigma_{11} &= (\sigma_E)_{11} - \frac{\varepsilon_0 \varepsilon_r U^2}{2\left(\lambda_t z_0\right)^2} \\ \sigma_{22} &= (\sigma_E)_{22} - \frac{\varepsilon_0 \varepsilon_r U^2}{2\left(\lambda_t z_0\right)^2} \\ \sigma_{33} &= (\sigma_E)_{33} + \frac{\varepsilon_0 \varepsilon_r U^2}{2\left(\lambda_t z_0\right)^2} \end{aligned}$$

From the abovementioned relations, it is apparent that the electrical term of the stress is only added in the thickness direction. This is because of the fact that the polarity of the Maxwell stress is positive only in the direction of the electric field [61] and in this case the electric field is applied in the thickness direction (σ_{33}).

Besides, the electrical force per unit area of the elastomer appears also as tractions on the major surfaces [6], such that:

$$\mathbf{n} \cdot \boldsymbol{\sigma}_M \cdot \mathbf{n} = \varepsilon_0 \varepsilon_r \frac{\tilde{E}^2}{2} \tag{4.53}$$

This behavior is depicted in Fig. 4.6

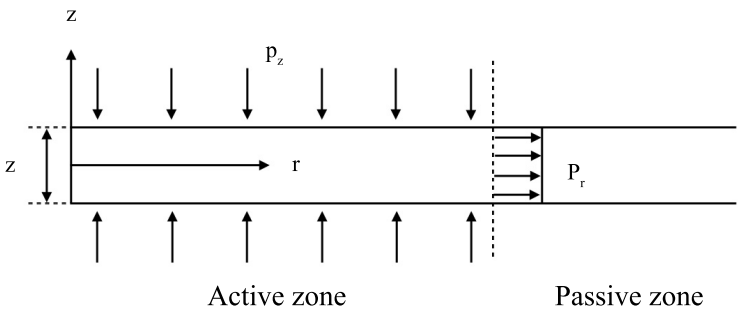

FIGURE 4.6: Out-of-plane pressure p_z and lateral stress p_r acting on the dielectric in a circular actuator, axisymmetric view [1]

4.6 Finite Element Implementation of Linear Viscoelasticity

4.6.1 Finite Element Formulation of a Nonlinear Problem

The starting point for the Finite Element (FE) implementation is the principle of "*Minimum Potential Energy*". The displacement field, $\mathbf{u}$ is determined such that the functional

$$\Pi(\mathbf{u}) = \int_\Omega \hat{\Psi}(\boldsymbol{\varepsilon}, \theta, \boldsymbol{\mathcal{I}})\, d\Omega - \int_\Omega \mathbf{u} \cdot \rho \mathbf{b}\, d\Omega - \int_{\partial\Omega} \mathbf{u}\boldsymbol{\varepsilon}\, d\partial\Omega \longrightarrow Min! \tag{4.54}$$

is minimized subjected to the essential boundary conditions (i.e. $\mathbf{u} = \bar{\mathbf{u}}$). In the context of small strains, the strain tensor, $\boldsymbol{\varepsilon}$, is defined by the following kinematic equation:

$$\boldsymbol{\varepsilon} := sym[\nabla \mathbf{u}] = \frac{1}{2}[\nabla \mathbf{u} + \nabla \mathbf{u}^T] \tag{4.55}$$

The variational formulation of Eq. (4.54) is obtained by the directional derivative (first variation of $\Pi(\mathbf{u})$):

$$\begin{aligned} G(\mathbf{u},\delta\mathbf{u}) &:= \delta\Pi = \frac{d}{d\epsilon}\Big|_{\epsilon\to 0}\Pi(\mathbf{u}+\epsilon\delta\mathbf{u}) = 0 \\ \Longrightarrow & \frac{d}{d\epsilon}\Big|_{\epsilon\to 0}\Big\{\int_\Omega \hat{\Psi}(sym[\nabla(\mathbf{u}+\epsilon\delta\mathbf{u})])\,d\Omega - \int_\Omega(\mathbf{u}+\epsilon\delta\mathbf{u})\cdot\rho\mathbf{b}\,d\Omega \\ & - \int_{\partial\Omega}(\mathbf{u}+\epsilon\delta\mathbf{u})\cdot\mathbf{t}\,d\partial\Omega\Big\} = 0 \end{aligned} \tag{4.56}$$

where ϵ is the eigenvalue.

Please note that $sym[\nabla(\mathbf{u}+\epsilon\delta\mathbf{u})] = \boldsymbol{\varepsilon} + \epsilon\delta\boldsymbol{\varepsilon}$. Then Eq. (4.56) can be written as:

$$G(\mathbf{u},\delta\mathbf{u}) = \int_\Omega \delta\boldsymbol{\varepsilon} : \partial_{\boldsymbol{\varepsilon}}\hat{\Psi}(\boldsymbol{\varepsilon},\theta,\boldsymbol{\mathcal{I}})\,d\Omega - \int_\Omega \delta\mathbf{u}\cdot\rho\mathbf{b}\,d\Omega - \int_{\partial\Omega}\delta\mathbf{u}\cdot\mathbf{t}\,d\partial\Omega \tag{4.57}$$

Equation (4.57) is the weak form of Eq. (4.54) which is called "*the Principle of Virtual Work*". Having the weak form at hand, it is now possible to continue with the FE discretization in matrix notation. Typically in FE implementation, the matrix notation is employed instead of the tensorial notation due to the efficient storage and computations. The weak form is written as:

$$G(\mathbf{u},\delta\mathbf{u}) = \int_\Omega \delta\boldsymbol{\varepsilon}^T\cdot\boldsymbol{\sigma}\,d\Omega - \int_\Omega \delta\mathbf{u}^T\cdot\rho\mathbf{b}\,d\Omega - \int_{\partial\Omega}\delta\mathbf{u}^T\cdot\mathbf{t}\,d\partial\Omega = 0 \tag{4.58}$$

where the Voigt-Notation as introduced in the previous sections is applied. Here no specification with respect to the type of element will be done. The following approximation of the displacement field in terms of the shape function $\mathbf{N}(\mathbf{u})$ and discrete nodal value, $\mathbf{d}$ is considered:

$$\mathbf{u}(\mathbf{x}) = \mathbf{N}(\mathbf{x})\cdot\mathbf{d} \quad ; \quad \delta\mathbf{u}(\mathbf{x}) = \mathbf{N}(\mathbf{x})\cdot\delta\mathbf{d} \tag{4.59}$$

from Eq. (4.59) the strain field is computed as:

$$\boldsymbol{\varepsilon}(\mathbf{x}) = \mathbf{B}(\mathbf{x})\cdot\mathbf{d} \quad ; \quad \delta\boldsymbol{\varepsilon}(\mathbf{x}) = \mathbf{B}(\mathbf{x})\cdot\delta\mathbf{d} \tag{4.60}$$

for a 2D problem, the $\mathbf{B}$-matrix has the following form:

$$\mathbf{B} = \left[\begin{array}{cc|cc|cc|cc} N_{1,x} & 0 & N_{2,x} & 0 & N_{3,x} & 0 & N_{4,x} & 0 \\ 0 & N_{1,y} & 0 & N_{2,y} & 0 & N_{3,y} & 0 & N_{4,y} \\ N_{1,y} & N_{1,x} & N_{2,y} & N_{2,x} & N_{3,y} & N_{3,x} & N_{4,y} & N_{4,x} \end{array}\right] \tag{4.61}$$

and the vector of nodal displacements looks like this:

$$\mathbf{d}^T = \begin{bmatrix} u_1 & v_1 & u_2 & v_2 & \cdots \end{bmatrix} \tag{4.62}$$

inserting Eq. (4.59) and (4.60) into Eq. (4.58) yields:

$$G(\mathbf{u}, \delta\mathbf{u}) = \delta\mathbf{d}^T \Big\{ \underbrace{\int_\Omega \mathbf{B}^T \cdot \boldsymbol{\sigma}\, d\Omega}_{\mathbf{f}_{int}} - \underbrace{\int_\Omega \mathbf{N}^T \cdot \rho\mathbf{b}\, d\Omega - \int_{\partial\Omega} \mathbf{N}^T \cdot \mathbf{t}\, d\partial\Omega}_{\mathbf{f}_{ext}} \Big\} = 0 \tag{4.63}$$

for arbitrary virtual displacements $\mathbf{d}^T$ one has:

$$\mathbf{f}_{int} = \mathbf{f}_{ext} \tag{4.64}$$

where,

$$\mathbf{f}_{int} = \int_\Omega \mathbf{B}^T \cdot \boldsymbol{\sigma}\, d\Omega = \prod_{e=1}^{n.Ele} \int_{\Omega_e} \mathbf{B}_e^T \cdot \boldsymbol{\sigma}\, d\Omega_e \tag{4.65}$$

$$\begin{aligned} \mathbf{f}_{ext} &= \int_\Omega \mathbf{N}^T \cdot \rho\mathbf{b}\, d\Omega + \int_{\partial\Omega} \mathbf{N}^T \cdot \mathbf{t}\, d\partial\Omega = \\ &\prod_{e=1}^{n.Ele} \Big\{ \int_{\Omega_e} \mathbf{N}_e^T \cdot \rho\mathbf{b}\, d\Omega_e + \int_{\partial\Omega_e} \mathbf{N}_e^T \cdot \mathbf{t}\, d\partial\Omega_e \Big\} \end{aligned} \tag{4.66}$$

for a general nonlinear problem, however, a residuum vector is defined as follows:

$$\mathbf{r}(\mathbf{d}) := \mathbf{f}_{int} - \mathbf{f}_{ext} = 0 \tag{4.67}$$

which is a set of nonlinear equations. We solve Eq. (4.67) using a typical Newton-Raphson scheme which requires the linearization of the residuum :

$$Lin\ \mathbf{r}(\mathbf{d})\Big|_{\mathbf{d}^i} = \mathbf{r}(\mathbf{d}^i) + \frac{\partial \mathbf{r}}{\partial \mathbf{d}}\Big|_{\mathbf{d}^i} (\mathbf{d}^{i+1} - \mathbf{d}^i) \stackrel{!}{=} \mathbf{0} \tag{4.68}$$

the solution of Eq. (4.68) gives the update for the nodal displacement $\mathbf{d}$.

$$\mathbf{d} = \mathbf{d} - (\mathbf{K}^i)^{-1} \mathbf{r}^i \tag{4.69}$$

with

$$\mathbf{r}^i = \mathbf{f}_{int}(\mathbf{d}^i) - \mathbf{f}_{ext} \tag{4.70}$$

and the tangent stiffness matrix $\mathbf{K}$:

$$\begin{aligned}\mathbf{K}^i =& \frac{\partial \mathbf{r}^i}{\partial \mathbf{d}} = \frac{\partial}{\partial \mathbf{d}} \mathbf{f}_{int}(\mathbf{d}^i) \\ =& \frac{\partial}{\partial \mathbf{d}} \int_\Omega \mathbf{B}^T \boldsymbol{\sigma} \, d\Omega \Big|_{\mathbf{d}^i} \\ =& \int_\Omega \mathbf{B}^T \frac{\partial \boldsymbol{\sigma}}{\partial \boldsymbol{\varepsilon}} \frac{\partial \boldsymbol{\varepsilon}}{\partial \mathbf{d}} \, d\Omega = \int_\Omega \mathbf{B}^T \mathbb{C} \mathbf{B} \, d\Omega \end{aligned} \tag{4.71}$$

4.6.2 Stress Updates and Constant Tangent Moduli

In this section the derivation of a local stress update algorithm for viscoelastic problems is elaborated which "lives" in a typical structural discretization at the integration points of a finite element mesh. For each one of the representations discussed earlier one could derive the algorithm in terms of either strain-like ($\boldsymbol{\alpha}_i$) or stress-like ($\boldsymbol{\beta}_i$) variables. Here, the numerical implementation of the **representation A** of linear viscoelasticity in terms of strain-like variables is considered. Such types of algorithms are the so-called deformation-driven algorithms and stresses are updated in the time interval of $[t_n, t_{n+1}]$, where:

1. All variables at time t_n are known.
2. The deformation, $\boldsymbol{\varepsilon}$, at time t_n is prescribed.
3. The internal variables (or history database) at time t_{n+1} has to be computed.

This is a typical set up of stress updates for local problems which is suitable for displacement type FE-implementation.

Recall the representation A of linear viscoelasticity:

$$\textbf{Representation A}: \begin{cases} \boldsymbol{\sigma} & = (\kappa e)\mathbf{I} + [2\mu_0 \boldsymbol{\varepsilon}' + \sum_{i=1}^n 2\mu_i(\boldsymbol{\varepsilon}' - \boldsymbol{\alpha}_i)] : \mathbb{P} \\ \boldsymbol{\beta}_i & = 2\mu_i(\boldsymbol{\varepsilon}' - \boldsymbol{\alpha}_i) \\ \dot{\boldsymbol{\alpha}}_i & = \frac{1}{\eta_i}\boldsymbol{\beta}_i \end{cases}$$

In a first step the evolution equation, $\dot{\boldsymbol{\alpha}}_i = \frac{1}{\eta_i}\boldsymbol{\beta}_i$, is integrated using a fully implicit backward Euler scheme, i.e. :

$$\begin{aligned}
\dot{\boldsymbol{\alpha}}^i_{n+1} &= \frac{\boldsymbol{\alpha}^i_{n+1} - \boldsymbol{\alpha}^i_n}{\Delta t} \\
\Longrightarrow \boldsymbol{\alpha}^i_{n+1} &= \boldsymbol{\alpha}^i_n + \Delta t\ \dot{\boldsymbol{\alpha}}^i_{n+1} \\
&= \boldsymbol{\alpha}^i_n + \Delta t\ \frac{1}{\eta_i}\boldsymbol{\beta}^i_{n+1} \\
&= \boldsymbol{\alpha}^i_n + \Delta t\ \frac{2\mu_i}{\eta_i}(\boldsymbol{\varepsilon'_{n+1}} - \boldsymbol{\alpha}^i_{n+1}) \\
&= \boldsymbol{\alpha}^i_n + \frac{\Delta t}{\tau_i}(\boldsymbol{\varepsilon'_{n+1}} - \boldsymbol{\alpha}^i_{n+1})
\end{aligned} \tag{4.72}$$

where $\tau_i = \dfrac{\eta_i}{2\mu_i}$ is the relaxation time.

Eq. (4.72) is a linear equation in $\boldsymbol{\alpha}^i_{n+1}$ due to the linear form of the considered model. Solving this for $\boldsymbol{\alpha}^i_{n+1}$ gives:

$$\boldsymbol{\alpha}^i_{n+1} = \frac{\boldsymbol{\alpha}^i_n + (\frac{\Delta t}{\tau_i})\boldsymbol{\varepsilon}'_{n+1}}{1 + \frac{\Delta t}{\tau_i}} \tag{4.73}$$

with this at hand the algorithmic stresses read:

$$\boldsymbol{\sigma}_{n+1} = (\kappa e_{n+1})\mathbf{I} + 2\mu_0\boldsymbol{\varepsilon}'_{n+1} + \sum_{i=1}^{n} 2\mu_i \left(\boldsymbol{\varepsilon}'_{n+1} - \frac{\boldsymbol{\alpha}^i_n + (\frac{\Delta t}{\tau_i})\boldsymbol{\varepsilon}'_{n+1}}{1 + \frac{\Delta t}{\tau_i}} \right) \tag{4.74}$$

the tangent moduli consistent with the chosen integration schemes are given by:

$$\mathbb{C}_{n+1} = \kappa\mathbf{I} \otimes \mathbf{I} + \left[2\mu_0 + \sum_{i=1}^{n} 2\mu_i \left(1 - \frac{\frac{\Delta t}{\tau_i}}{1 + \frac{\Delta t}{\tau_i}} \right) \right] : \mathbb{P} \tag{4.75}$$

The abovementioned algorithm can now be summarized as follows:

1. Given is the database $\{\boldsymbol{\varepsilon}, \mathbf{H}\}$ at time t_n and current deformation $\boldsymbol{\varepsilon}_{n+1}$ at time $t_n + \Delta t$ with $\mathbf{H} = \{\boldsymbol{\alpha}^i, \cdots, \boldsymbol{\alpha}^n\}$

2. Decompose strain into volumetric, $e_{n+1} := tr[\boldsymbol{\varepsilon}_{n+1}]$ and isochoric parts, $\boldsymbol{\varepsilon}'_{n+1} := dev[\boldsymbol{\varepsilon}_{n+1}]$

3. Set the algorithmic parameters and update history variables:

3.1 Set the algorithmic parameters as:

$$C_1^i := \frac{\Delta t}{\tau_i} \quad ; \quad C_2^i := 1 - \frac{\frac{\Delta t}{\tau_i}}{1 + \frac{\Delta t}{\tau_i}} = \frac{1}{1 + C_1^i}$$

3.2 Update History variables:

$$\boldsymbol{\alpha}_{n+1}^i = \frac{\boldsymbol{\alpha}_n^i + (\frac{\Delta t}{\tau_i})\boldsymbol{\varepsilon}'_{n+1}}{1 + \frac{\Delta t}{\tau_i}}$$

and store $\mathbf{H}_{n+1} = \{\boldsymbol{\alpha}_{n+1}^i, \cdots, \boldsymbol{\alpha}_{n+1}^n\}$

4. Compute stresses:

$$\boldsymbol{\sigma}_{n+1} = (\kappa e_{n+1})\mathbf{I} + 2\mu_0 \boldsymbol{\varepsilon}'_{n+1} + \sum_{i=1}^{n} 2\mu_i \left(\boldsymbol{\varepsilon}'_{n+1} - \frac{\boldsymbol{\alpha}_n^i + (\frac{\Delta t}{\tau_i})\boldsymbol{\varepsilon}'_{n+1}}{1 + \frac{\Delta t}{\tau_i}} \right)$$

5. Compute constant tangent moduli:

$$\mathbb{C}_{n+1} = \kappa \mathbf{I} \otimes \mathbf{I} + \left[2\mu_0 + \sum_{i=1}^{n} 2\mu_i \left(1 - \frac{\frac{\Delta t}{\tau_i}}{1 + \frac{\Delta t}{\tau_i}} \right) \right] : \mathbb{P}$$

4.6.3 Addition of the Maxwell Stress in the Material Model

Using the abovementioned stress-update algorithm one ends up only with elastic stresses. The Cauchy stress tensor of an activated DE, however, contains, in addition, the components of Maxwell stresses. As such, it is assumed that the Maxwell stresses can be regarded as initial stresses in the system. Elastic stresses calculated thereafter using the aforementioned stress-update algorithm is simply added to the pre-existing stress components which finally result in the complete description of the stresses in the system.

4.6.4 Implementation of the Algorithm in ABAQUS

ABAQUS general FE code is used in the present study. The reason why ABAQUS has been chosen is ABAQUS's capability to tailor to one 's specific analysis requirements through the usage of "user subroutines". A complete list of such routines along with the usage, general interfaces and requirements can be found in Ref. [71, 72].

Developing such routines requires a basic knowledge of FORTRAN programming language. In the present study three user subroutines have been exploited; The first one of which is a user subroutine called "**SDVINI**" used to define and initialize the history variables associated with the stress-update algorithm, the second subroutine called "**SIGINI**" is used to initialize the stress tensor and "**UMAT**" user subroutine is used to implement the stress-update algorithm of linear viscoelastic material model. The convergence of UMAT subroutine depends on the definition of the Jacobian of the routine known as DDSDDE. It corresponds to the constant tangent moduli as defined in Sec. 4.6.2. The Appendix A contains the subroutines used in the present study.

Using such subroutines demands inclusion of specific ABAQUS "Keywords" in the input file as following:

1. The Keywords to use the UMAT:

   ```
   *MATERIAL, NAME = <USER>
   *USER MATERIAL, CONST = <number of constants>
   <constants>
   ```

2. The Keywords to use SDVINI:

   ```
   *DEPVAR
   <number of solution dependent variables>,
   *INITIAL CONDITIONS,TYPE=SOLUTION,USER
   ```

3. The Keywords to use SIGINI:

   ```
   *INITIAL CONDITIONS,TYPE=STRESS,USER
   ```

Chapter 5

Numerical Simulation of Dielectric Elastomers

5.1 General overview

In this chapter the results of the FE simulation of actuation principles of a circular DE using ABAQUS FE code are presented. First the verification of the developed user material subroutine for ABAQUS (UMAT), then the demonstration of a model problem for DEs are presented. The model problem is the one discussed in Ref. [1]. The details regarding the model are found in the respective section. The ultimate goal of introducing such a model problem is to develop a benchmark using which, one is further able to examine the developed material routine and observe the potential shortcomings. In this fashion the model is first simulated using ABAQUS material library and then with the UMAT.

5.2 UMAT Verification

How a UMAT was developed and further verified is presented in this section. It was first attempted to implement the previously mentioned stress-update algorithm of linear viscoelasticity (representation A) in ABAQUS as a user material subroutine (UMAT). This UMAT is presented in Appendix A. The verification

example was a small-strain time domain viscoelasticity with elastic material properties (example 2.2.2 ABAQUS Verification Manual [73]). The verification of the developed UMAT, however, was not successful.

Due to the unsuccessful attempt the author later borrowed and modified an already developed UMAT for a linear viscoelastic material. This was a subroutine developed by Prof. R. M. Hackett - University of Mississippi in 1999 [74]. This UMAT is presented in Appendix A. It is based on Maxwell elements in parallel with an elastic spring (Fig. 4.5) and the convolution representation of viscoelasticity. The algorithm of this routine can be found in Ref. [14]. In this section the verification results of this UMAT versus the already mentioned ABAQUS example are described.

ABAQUS employs the so-called Prony series to model a viscoelastic problem in conjunction with elastic (hyperelastic) properties. This requires the knowledge of Prony series coefficient as well as the elastic properties of the material. The UMAT presented here, however, demands exploitation of a different form of material properties and a conversion is needed to obtain the properties suitable for the UMAT. These two types of properties are given in Table. 5.1.

TABLE 5.1: Material properties for UMAT verification

ABAQUS	**UMAT**
Young's modulus (E) = 30 MPa	Bulk modulus (κ)= 50 MPa
Poisson's ratio = 0.4	Ground shear modulus (μ_∞) = 10.714 MPa
$\bar{g}_1^p = 0.25$	$\mu_1 = 2.6785$ MPa
$\bar{k}_1^p = 0.25$	-
$\tau_1 = 5$ s	$\tau_1 = 5$ s
$\bar{g}_2^p = 0.25$	$\mu_2 = 2.6785$ MPa
$\bar{k}_2^p = 0.25$	-
$\tau_2 = 10$ s	$\tau_2 = 10$ s

The abovementioned conversion is done as following; to obtain the bulk modulus, κ, one can plug the Young's Modulus, E, and Poisson's ratio, ν, into this expression:

$$\kappa = \frac{E}{3\,(1-2\nu)} \tag{5.1}$$

The ground shear modulus can be obtained as:

$$\mu_\infty = \frac{E}{2\,(1+\nu)} \tag{5.2}$$

The Prony series coefficients, $\bar{g}_i^p$, are dimensionless shear modulus, the sum of which with the dimensionless ground shear modulus must be one. Hence the dimensionless ground shear modulus is obtained as:

$$\bar{g}_\infty^p = 1 - \sum_{i=1}^{N} \bar{g}_i^p \tag{5.3}$$

Using,

$$\bar{g}_\infty^p = \frac{\mu_\infty}{\mu_0} \longrightarrow \mu_0 = \frac{\mu_\infty}{\bar{g}_\infty^p} \tag{5.4}$$

One obtains the instantaneous ground shear modulus, μ_0. If the instantaneous material properties are desired, then,

$$\mu_i = \mu_0 \ . \ \bar{g}_i^p \tag{5.5}$$

otherwise,

$$\mu_i = \mu_\infty \ . \ \bar{g}_i^p \tag{5.6}$$

As mentioned earlier the verification attempt of the UMAT based on "representation A" was unsuccessful and another UMAT was used instead which was successfully verified against ABAQUS verification example. The verification results are given in Table. 5.2 where minimum and maximum principal stress in two models are compared. There are, however, some discrepancies between the obtained results which are deemed to be due to the inaccurate material data and a calibration of material properties is necessary.

TABLE 5.2: UMAT verification results

ABAQUS	**UMAT**
Max. Principal Stress (MPa) = 20.8	Max. Principal Stress (MPa) = 34.5
Min. Principal Stress (MPa) = $2.2 \ . \ 10^{-10}$	Min. Principal Stress (MPa) = $2.4 \ . \ 10^{-10}$

5.3 Model Problem

5.3.1 General Overview

The model problem as explained in Ref. [1] is a circular DE made of acrylic elastomer VHB 4910 with the radius of $r_0 = 14\ mm$ and a thickness of $z_0 = 60\ \mu m$ after pre-stretching by a factor of $\lambda_p = 4$. Both surfaces of the DE are coated with compliant electrode. The radius of the coated area is $r_{el} = 7\ mm$, see Fig. 5.1. The elastic and viscoelastic properties of a pre-stretched dielectric are given in Table. 5.3 which are the results of a relaxation test [48]. For simplicity the DE is assumed to be axisymmetric around y-axis.

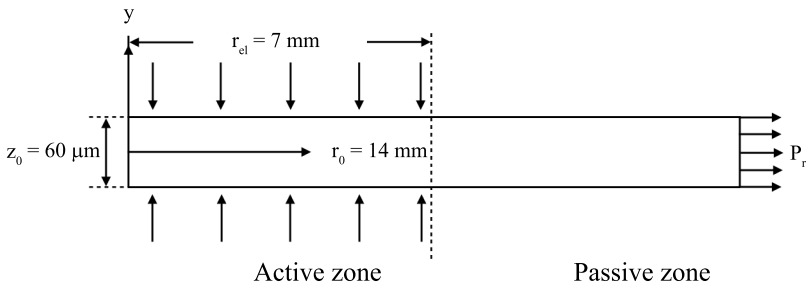

FIGURE 5.1: Two dimensional model problem [1]

TABLE 5.3: DE properties from a relaxation test [48]

Yeoh Model Coefficients
C_{10}(MPa) = 0.0803
C_{20} (MPa) = -7.65 . 10^{-4}
C_{30} (MPa) = 9.84 . 10^{-6}
Prony Series Coefficients
$\bar{g}_1^p = 0.570$
$\tau_1 = 0.311$ s
$\bar{g}_2^p = 0.189$
$\tau_2 = 3.35$ s
$\bar{g}_3^p = 0.0860$
$\tau_3 = 35.7$ s
$\bar{g}_4^p = 0.0543$
$\tau_4 = 370$ s

As explained by Wissler and Mazza [48] two main challenges to simulate the actuation of a DE are (1) inclusion of the Maxwell stress in the system and (2) determination of the constitutive equations.

To address the first difficulty two approaches was employed to include the Maxwell stress in the system. In the first approach the Maxwell stress was applied through a lateral pressure (p_r) along with the tractions on both sides of the DE. The Maxwell stress was computed according to Eq. 4.52 and was then applied as a uniform pressure on the lateral surfaces of the DE. The tractions were computed using Eq. 4.53 and then applied as uniform pressures on the electrode surfaces.

In the second approach, the Maxwell stress was assumed as a residual stress (pre-stress) in the system and was applied using an ABAQUS user subroutine called "SIGINI". The way the tractions were enforced in the system remained unchanged in this approach.

Either approaches used the current thickness of the DE to compute the Maxwell stress. As such, one had to know the stretch ratio in the thickness direction (λ_t[1]) to get the current thickness. As stated in Ref. [48], one expects $10\% \approx 30\%$ increase in length (elongation) when the DEs is activated. Since the stretch ratio in the thickness direction was unknown, a series of trials were run to calibrate the amount of stretch ratio which gave the $10\% \approx 30\%$ elongation upon activation of the DE.

Another aspect which is discussed in this section is the usage of ABAQUS material library versus the developed UMAT. A hyper-viscoelastic material model was used from ABAQUS material library. The hyperelastic part was based on Yeoh hyperelastic model [52] and the viscoelastic part was based on the time domain Prony series. The results obtained with the ABAQUS material library was used as a benchmark to determine if the developed UMAT was accurate enough for the sake of simulation.

In the following sections, first a series of trials was carried out to find the stretch ratio of the DE. After obtaining the stretch ratio three cases were tested with only tractions, lateral pressure/pre-stress and both tractions and lateral pressure/pre-stress in the system. The effect of applied voltage on the actuation of DEs was further investigated. Finally a comparison was made between the UMAT and ABAQUS material library.

[1]The ratio between the thickness in the current configuration, z_0, and the thickness in the reference configuration, z.

5.3.2 Calibrating the Stretch Ratio

As explained in Sec. 4.5.3 the contribution of the Maxwell stress to the total stress comes from:

$$\mp \frac{\varepsilon_0 \varepsilon_r U^2}{2\left(\lambda_t z_0\right)^2}$$

The only unknown parameter in the abovementioned expression is the stretch ratio in the thickness direction, λ_t. By applying a constant voltage of 3 kV the stretch ratio which produced 30% elongation was determined. Both approaches of applying Maxwell stress were used here, although the second approach i.e. using pre-stress in the systems deemed to be the correct one. Table. 5.4 and Table. 5.5 summarize the calibration results of the stretch ratio using the lateral pressure approach and pre-stress approach, respectively.

TABLE 5.4: Calibration results of the stretch ratio using the lateral pressure approach

Stretch Ratio (λ_t)	0.5	0.4	0.3	0.26
Traction (MPa)	0.052	0.052	0.052	0.052
Maxwell Stress (MPa)	0.208	0.325	0.577	0.7691
Elongation (mm)	0.6652	1.01	1.426	1.275[&]

[&] The analysis did not converge

TABLE 5.5: Calibration results of the stretch ratio using pre-stress approach

Stretch Ratio (λ_t)	0.5	0.4	0.3	0.26
Traction (MPa)	0.052	0.052	0.052	0.052
Maxwell Stress (MPa)	0.208	0.325	0.577	0.7691
Elongation (mm)	1.01	1.66	2.77	4.261

While the modeled DE had a radius of 14 mm, the 30% of that was around 4.2 mm; having said that, the stretch ratio of 0.26 with applied voltage of 3 kV created such an elongation.

5.3.3 Test Cases

Adopting the pre-stress approach to include the Maxwell stress in the system, the cases where, (1) only tractions were present in the system, (2) only Maxwell stresses were present in the system and (3) tractions and Maxwell stresses were

both present in the system, were examined in this section. The results of such a comparison are shown in Table. 5.6. As the results suggest, the inclusion of both tractions and Maxwell stress was the only case which more closely mimicked the actuation of real DEAs.

TABLE 5.6: Test cases of Maxwell Stress inclusion in the system

Test Case 1	Elongation (mm) = 0.01875
Test Case 2	Elongation (mm) = 4.189
Test Case 3	Elongation (mm) = 4.241

5.3.4 Effect of Varying Applied Voltage on the Activation

This section intends to compare the effect of applied voltage on the increased length of activated DE. To that end, with the stretch ratio of 0.26, the voltages of 1 kV, 1.5 kV, 2 kV, 2.5 kV, and 3 kV were applied to the system. The obtained elongation are summarized in Table. 5.7. As the results indicate to obtain the elongation of $10\% \approx 30\%$, the applied voltage had to be in the range of 2 kV $\approx$ 3 kV.

TABLE 5.7: Effect of applied voltage, U, on the elongation of DE

Applied Voltages (kV)	1	1.5	2	2.5	3
Traction (MPa)	0.0058	0.0130	0.0231	0.0361	0.052
Maxwell Stress (MPa)	0.0855	0.1923	0.3418	0.5341	0.7691
Elongation (mm)	0.189	0.902	1.67	2.755	4.241

5.3.5 Application of UMAT

One of the primary goals of the current study was to develop a material routine which was able to simulate the actuation principles of the DEs. Using the UMAT verified in Sec. 5.2, the FE simulation of DEs is sought in this section. Both approaches of using pre-stress and lateral pressures were used herein. With the applied voltage of 3 kV and the stretch ratio of 0.26, one obtains the results presented in Table. 5.8. For the sake of comparison the results obtained with ABAQUS viscoelasticity and ABAQUS hyper-viscoelasticity are also presented in this table. The material properties for DE which are the converted values of the previousely mentioned relaxation test (Table 5.3) are given in Table. 5.9.

Table 5.8: Results of DE actuation simulation with UMAT, ABAQUS Viscoelasticity and ABAQUS Hyper-viscoelasticity

UMAT and Lateral Pressure(p_r)	Elongation (mm)= 0.488*
ABAQUS Viscoelasticity and Lateral Pressure(p_r)	Elongation (mm)= 0.0631
ABAQUS Hyper-viscoelasticity and Lateral Pressure(p_r)	Elongation (mm)= 1.24*
UMAT and Pre-stress	Elongation (mm)= 0.47
ABAQUS Viscoelasticity and Pre-stress	Elongation (mm)= 0.09
ABAQUS Hyper-viscoelasticity and Pre-stress	Elongation (mm)= 4.24

* The analysis did not converge

Table 5.9: DE material properties for UMAT

Elastic Properties
Young's Modulus (MPa) = 18.42
Poisson's ratio (MPa) = 0.49
Bulk modulus (MPa) = 307
Ground shear modulus (MPa) = 6.14
Viscoelastic Properties
μ_1 (MPa) = 3.5
τ_1 (s) = 0.311
μ_2 (MPa) = 1.16
τ_2 (s) = 3.35
μ_3 (MPa) = 0.0860
τ_3 (s) = 35.7
μ_4 (MPa) = 0.0543
τ_4 (s) = 370

It was observed that using the pre-stress approach, the obtained results were not satisfactory. With the other approach i.e. lateral pressure, the elongation was observed but not as much as expected. As the lateral pressure increased the analysis was aborted half-way through. For the sake of comparison, the elastic and viscoelastic material models of ABAQUS material library were also used to compare the results. It not only did not show any improvements, but the obtained elongation was even lower than the one obtained with UMAT. It can be then concluded that the linear viscoelastic material routine was definitely insufficient to simulate the actuation of a DE. In the following section the recommendations to remedy this problem will be presented.

5.3.6 Three Dimensional Extension

In this section the three dimensional extension of the model problem with the same geometry data and material properties will be presented, see Fig. 5.2.

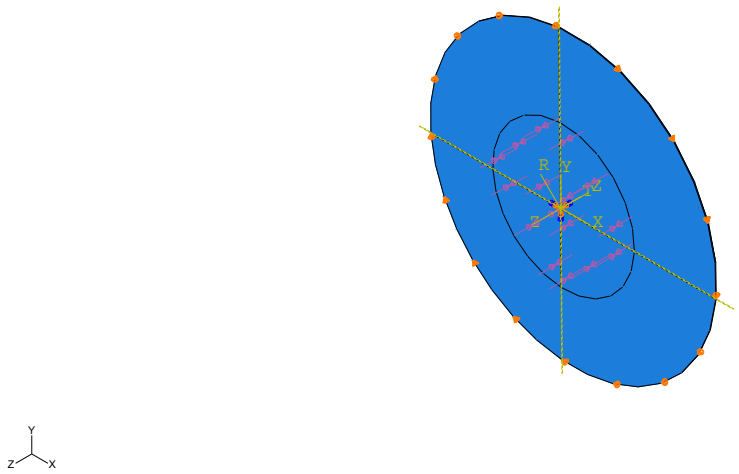

FIGURE 5.2: Three dimensional model problem

For this model the Maxwell stress was included using the pre-stress approach. Assuming the stretch ratio of $\lambda_t = 0.26$, the actuation was simulated with the applied voltages of 2 kV, 2.5 kV, and 3 kV. The resulting tractions and stresses were those given in Table. 5.7.

The ABAQUS material library was used to run the simulation. The activated DE with 3 kV applied voltage is illustrated in Fig. 5.3.

Table. 5.10 presents the obtained results for actuation simulation of DE using both ABAQUS material library. For comparison, the 2D results are also presented in this table.

TABLE 5.10: Results of 3D DE actuation simulation

Applied Voltage U (kV)	**3D Elongation(mm)**	**2D Elongation(mm)**
2	0.9714	1.67
2.5	1.482	2.76
3	2.069	4.24

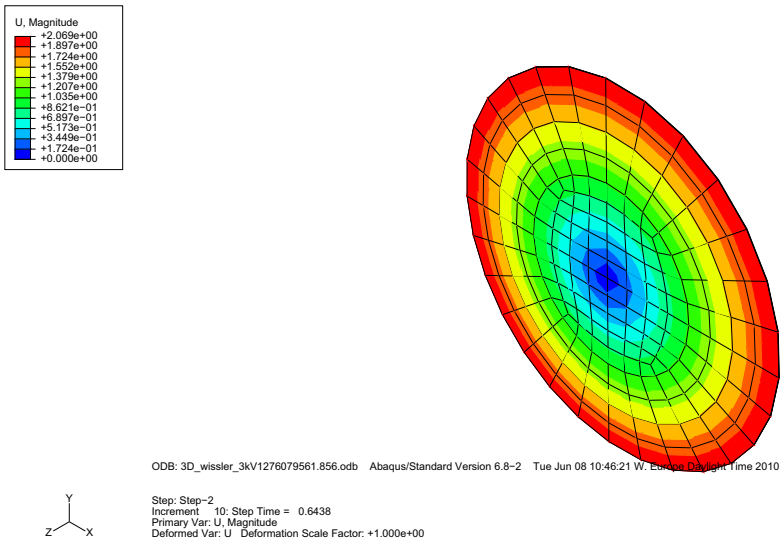

FIGURE 5.3: Activate DE with 3 kV

One can observe some discrepancies between these set of results and those elaborated in the previous section. According to Eq. (4.52) the Maxwell stress in the three dimensional case is added to σ_{33} while it is subtracted from σ_{11} and σ_{22}. It is assumed here that for the two dimensional problem the Maxwell stress is added to σ_{22} and subtracted from σ_{11}. Therefore in the three dimensional case there is one extra negative component which could explain the discrepancy between the two and three dimensional results.

Another reasone coule be the fact that for the previous model the reduced integration elements were used which are usually less stiff.

The stretch ratio which was calibrated for the previously 2D problem was also used here. Perhaps another calibration for the stretch ratio for the 3D model is also required in order to improve the results.

Chapter 6

Conclusion and Outlook

The objective of the current study was to investigate the viscoelastic behavior of DEAs using the Finite Element Method. To that end a linear viscoelastic material routine was implemented in ABAQUS Finite Element code as a user subroutine. To account for the stresses induced by the electric field, the stress tensor was initiated with some pre-stresses based on the work of Goulbourne et al. [6].

Two model problems were introduced to be served as a benchmark to verify the results obtained with the linear viscoelastic material model. The visco-hyperelastic material model was exploited for these two models. It was then concluded that:

- The linear viscoelastic material model was insufficient to correctly simulate the actuation of DE.
- To obtain the elongation of 10% $\approx$ 30%, the applied voltage must be in the range of 2 kV $\approx$ 3 kV.
- To correctly simulate the actuation of DE one should consider both tractions on the surfaces of DE and the Maxwell stresses induced by electric field.
- To find the correct value of Maxwell stress one should know the correct stretch ratio in the direction of applied voltage.

Based on the obtained results the following set of actions are recommended:

- To further enhance the simulation of DEs and obtain a more realistic result, the use of hyperelastic material model is recommended.

- It is also suggested to implement the material routine with the Maxwell stresses included in the routine as the electric free term similar to the work of Zhao and Suo [2].

- For the current work the radial DEs were used. Simulation of other configurations is recommended.

- Conducting a parametric study is also suggested proceeded by an optimization to find the optimal configuration of DEs. Needless to say, one should decide on the proper design variables, objective function and constraints prior to setting up the optimization problem.

Appendix A

User Subroutines

A.1 UMAT for Representation A

The following subroutine is the modified version of a routine originally written in C++. It was developed at the Institute of Applied Mechanics (Chair I), university of Stuttgart to be used in conjunction with *FEAPpv* finite element program. FEAPpv is a general purpose finile element analysis program designed for research and educational use by Robert L. Taylor. The source code and manuals for FEAPpv are available at `http://www.ce.berkeley.edu/projects/feap/feappv`. The program is described in Ref. [65]. As mentioned in chapter four, it has been developed for linear viscoelasticity in terms of internal variable. The corresponding generalized Maxwell model consists of two Maxwell elements in parallel with an elastic spring (N = 2).

```
C **********************************************************************
      SUBROUTINE SDVINI(STATEV,COORDS,NSTATV,NCRDS,NOEL,NPT,LAYER,KSPT)
C
      INCLUDE 'ABA_PARAM.INC'
C
      DIMENSION STATEV(NSTATV),COORDS(NCRDS)
      INTEGER I
C
      DO I=1,NSTATV
        STATEV(I)=0.0D0
```

```
      END DO
C      WRITE(6,*)'SDVINI-STATEV',(STATEV(IXX),IXX=1,6)
      RETURN
      END
C ***********************************************************************
      SUBROUTINE UMAT(STRESS,STATEV,DDSDDE,SSE,SPD,SCD,
     1 RPL,DDSDDT,DRPLDE,DRPLDT,
     2 STRAN,DSTRAN,TIME,DTIME,TEMP,DTEMP,PREDEF,DPRED,CMNAME,
     3 NDI,NSHR,NTENS,NSTATV,PROPS,NPROPS,COORDS,DROT,PNEWDT,
     4 CELENT,DFGRD0,DFGRD1,NOEL,NPT,LAYER,KSPT,KSTEP,KINC)
C
      INCLUDE 'ABA_PARAM.INC'
C
      CHARACTER*80 CMNAME
      DIMENSION STRESS(NTENS),STATEV(NSTATV),DDSDDE(NTENS,NTENS),
     1 DDSDDT(NTENS),DRPLDE(NTENS),STRAN(NTENS),DSTRAN(NTENS),
     2 TIME(2),PREDEF(1),DPRED(1),PROPS(NPROPS),COORDS(3),DROT(3,3),
     3 DFGRD0(3,3),DFGRD1(3,3)
C
         REAL II(NTENS,NTENS), PP(NTENS,NTENS), DEV(NTENS)
         REAL e, fact1_1, fact2_1, fact1_2, fact2_2
         REAL TOTAL
         INTEGER I1, I2, I3, I4, I5, J1, K1
         INTEGER K2, K3, K4
C
C Definition of identity tensor II
      DO I1=1,3
       DO I2=1,3
         II(I1,I2)=1.0
       END DO
      END DO
      DO I1=4,6
       DO I2=1,3
         II(I1,I2)=0.0
       END DO
      END DO
```

```
      DO I1=1,6
       DO I2=4,6
         II(I1,I2)=0.0
       END DO
      END DO
C Definition of projectory tensor PP
      DO I3=4,6
       DO I4=1,3
         PP(I3,I4)=0.0
       END DO
      END DO
      DO I3=1,3
       DO I4=4,6
         PP(I3,I4)=0.0
       END DO
      END DO
      PP(1,2)=0.0
      PP(1,3)=0.0
      PP(2,1)=0.0
      PP(2,3)=0.0
      PP(3,1)=0.0
      PP(3,2)=0.0
      PP(4,5)=0.0
      PP(4,6)=0.0
      PP(5,4)=0.0
      PP(5,6)=0.0
      PP(6,4)=0.0
      PP(6,5)=0.0
      PP(1,1)=2.0/3.0
      PP(2,2)=2.0/3.0
      PP(3,3)=2.0/3.0
      PP(4,4)=0.5
      PP(5,5)=0.5
      PP(6,6)=0.5
C
C  Definition of the trace of strains
```

```
C
      e = STRAN(1)+STRAN(2)+STRAN(3)
C
C  Definition of deviator of strains
C
         DO I5=1,3
           DEV(I5)=STRAN(I5)-e/3
         END DO
         DO I5=4,NTENS
           DEV(I5)=STRAN(I5)
         END DO
C
C Definition of the algorithmic parameters
C
! mu1= PROPS(3), eta1=PROPS(4)
! mu2=PROPS(5), eta2=PROPS(6)
!C
         fact1_1=2.0*PROPS(3)*DTIME/PROPS(4)
         fact2_1=1.0/(1.0+fact1_1)
C
         fact1_2=2.0*PROPS(5)*DTIME/PROPS(6)
         fact2_2=1.0/(1.0+fact1_2)
C
C Updating history
C
         DO J1=1,6
           STATEV(J1) = (STATEV(J1)+fact1_1*DEV(J1))/(1.0+fact1_1)
         END DO
C
         DO J1=7,12
           STATEV(J1) = (STATEV(J1)+fact1_2*DEV(J1))/(1.0+fact1_2)
         END DO
C
C Computing stress
C
         DO K1=1,3
```

```
            STRESS(K1)=PROPS(1)*e+2.0*PROPS(2)*DEV(K1)+
     1               2.0*PROPS(3)*(DEV(K1)+STATEV(K1))+
     2               2.0*PROPS(5)*(DEV(K1)+STATEV(K1+6.0))
!     2                2.0*PROPS(5)*(DEV(K1)+STATEV(K1+6.0))
          END DO
C
          DO K2=4,NTENS
            STRESS(K2)=2.0*PROPS(2)*DEV(K2)+
     1                2.0*PROPS(3)*(DEV(K2)+STATEV(K2))+
     2                2.0*PROPS(5)*(DEV(K1)+STATEV(K1+6.0))
!     2                 2.0*PROPS(5)*(DEV(K1)+STATEV(K1+6.0))
          END DO
C
C Compute moduli or jacobian
          TOTAL=PROPS(3)*fact2_1 + PROPS(5)*fact2_2
C
          DO K3=1,NTENS
            DO K4=1,NTENS
              DDSDDE(K3,K4)=PROPS(1)*II(K3,K4)+2.0*(PROPS(2)+
     1                     TOTAL)*PP(K3,K4)
            END DO
          END DO
       RETURN
       END
C
C ***************************************************************************
```

A.2 UMAT Developed by Prof. R. M. Hacket

This subroutine was originally developed by Prof. R. M. Hackett at the department of civil engineering, university of Mississippi [74]. It is based on the generalized Maxwell Model. The original code was based on four Maxwell elements (N = 4) in parallel with an elastic spring. Here the modified version for N = 2 and N = 4 are presented. The corresponding algorithm can be found in Ref. [14].

A.2.1 UMAT with Two Maxwell Elements (N = 2)

```
C ************************************************************
C *
C *                          U M A T
C *
C *      AN ABAQUS USER MATERIAL MODEL FOR 3D VISCOELASTICITY
C * (BASED ON MAXWELL ELEMENTS IN PARALLEL WITH AN ELASTIC SPRING)
C *
C *
C *  WRITTEN BY : Prof. R. M. Hackett - University of Mississippi
C *                    DATE : SPRING 1999
C *  REVISED BY : CHRIS L. MULLEN- University of Mississippi
C *                    DATE : SPRING 1999
C *  LAST REVISED BY : Abdolhamid Attaran
C *                DATE : Last Rev. Date April 2010
C *
C ************************************************************
C23456789012345678901234567890123456789012345678901234567890123456789012
       SUBROUTINE UMAT (STRESS,STATEV,DDSDDE,SSE,SPD,SCD,
     1 RPL,DDSDDT,DRPLDE,DRPLDT,
     2 STRAN,DSTRAN,TIME,DTIME,TEMP,DTEMP,PREDEF,DPRED,CMNAME,
     3 NDI,NSHR,NTENS,NSTATV,PROPS,NPROPS,COORDS,DROT,PNEWDT,
     4 CELENT,DFGRD0,DFGRD1,NOEL,NPT,LAYER,KSPT,KSTEP,KINC)
C
        INCLUDE 'ABA_PARAM.INC'
C
        CHARACTER*8 CMNAME
```

```
        DIMENSION STRESS(NTENS),STATEV(NSTATV),
     1 DDSDDE(NTENS,NTENS),DDSDDT(NTENS),DRPLDE(NTENS),
     2 STRAN(NTENS),DSTRAN(NTENS),TIME(2),PREDEF(1),DPRED(1),
     3 PROPS(NPROPS),COORDS(3),DROT(3,3),DFGRD0(3,3),DFGRD1(3,3)
       DIMENSION DSTRES(6),D(3,3)
C
C  PROPS(1) through PROPS(3) are shear modulus values in Pa
C       PROPS(1) = 9.440e8
C       PROPS(2) = 1.738e8
C       PROPS(3) = 5.212e8
C  PROPS(4) & PROPS(5) are relaxation times in seconds
C       PROPS(4) = 1.366e-4
C       PROPS(5) = 1.366e-5
C  PROPS(6) is the bulk modulus in Pa
C       PROPS(6) = 7.009e9
C  DIMENSION VARIABLES THAT ARE INTERNAL TO SUBROUTINE
        DIMENSION SM1OLD(6),SM2OLD(6), SM1(6),SM2(6),
     1            SM1DOT(6),SM2DOT(6)
       WRITE(6,*)'THIS IS A TEST'
       WRITE(6,*) NDI, NSHR, NTENS, NSTATV, NPROPS
       DO I = 1,6
          SM1OLD(I) = STATEV(I)
       END DO
       DO I = 1,6
          SM2OLD(I) = STATEV(I+6)
       END DO
       GM = PROPS(1) + PROPS(2) + PROPS(3)
C  EVALUATE NEW STRESS TENSOR
       EV = 0.
       DEV = 0.
       DO K1 = 1,NDI
          EV = EV + STRAN(K1)
          DEV = DEV + DSTRAN(K1)
       END DO
C
C
```

```
      CALL MAXWEL(SM1OLD,SM2OLD,SM1,SM2,
     1            SM1DOT,SM2DOT,
     2            DTIME,PROPS,NPROPS,STRAN,NTENS)
      TERM1 = PROPS(6) - 2.0*GM/3.0
      TERM2 = 2.0*GM
C
C
      DO K1 = 1,NDI
         DSTRES(K1) = TERM1*DEV + TERM2*DSTRAN(K1) -
     1               2.0*(PROPS(4)*SM1DOT(K1) +
     2                    PROPS(5)*SM2DOT(K1)) +
     3               2.0*TERM1*EV + 2.0*TERM2*STRAN(K1) - 2.0*STRESS(K1)
         STRESS(K1) = STRESS(K1) + DSTRES(K1)
      END DO
C
      WRITE(6,1000) (STRESS(i),i=1,NDI)
 1000 FORMAT(6(1pe12.3))
C     STOP
C
      I1 = NDI
C
      DO K1 = 1,NSHR
         I1 = I1 + 1
         DSTRES(I1) = (TERM2/2.0)*DSTRAN(I1) -
     1               2.0*(PROPS(4)*SM1DOT(I1) +
     2                    PROPS(5)*SM2DOT(I1)) +
     3               2.0*(TERM2/2.0)*STRAN(I1) - 2.0*STRESS(I1)
         STRESS(I1) = STRESS(I1) + DSTRES(I1)
      END DO
C
C  CREATE NEW JACOBIAN
C
      DO K1 = 1,NTENS
         DO K2 = 1,NTENS
            DDSDDE(K2,K1) = 0.
         END DO
```

```
      END DO
C
      DO K1 = 1,NDI
         DDSDDE(K1,K1) = TERM1 + TERM2
      END DO
C
      DO K1 = 2,NDI
         N2 = K1 - 1
         DO K2 = 1,N2
            DDSDDE(K2,K1) = TERM1
            DDSDDE(K1,K2) = TERM1
         END DO
      END DO
C
      I1 = NDI
C
      DO K1 = 1,NSHR
         I1 = I1 + 1
         DDSDDE(I1,I1) = TERM2/2.0
      END DO
C
C  COMPUTE CHANGE IN SPECIFIC TOTAL ENERGY
C
      TDE = 0.
C
      DO K1 = 1,NTENS
         TDE = TDE + (STRESS(K1) + .5*DSTRES(K1))*
     1         DSTRAN(K1)
      END DO
C
C  COMPUTE CHANGE IN SPECIFIC ELASTIC STRAIN ENERGY
C
      DO K1 = 1,NDI
         D(K1,K1) = TERM1 + TERM2
      END DO
C
```

```
      DO K1 = 2,NDI
         N2 = K1 - 1
         DO K2 = 1,N2
            D(K1,K2) = TERM1
            D(K2,K1) = TERM1
         END DO
      END DO
C
      DEE = 0.
C
      DO K1 = 1,NDI
         TERM1 = 0.
         TERM2 = 0.
         DO K2 = 1,NDI
            TERM1 = TERM1 + D(K1,K2)*STRAN(K2)
            TERM2 = TERM2 + D(K1,K2)*DSTRAN(K2)
         END DO
         DEE = DEE + (TERM1 + .5*TERM2)*DSTRAN(K1)
      END DO
C
      I1 = NDI
C
      DO K1 = 1,NSHR
         I1 = I1 + 1
         DEE = DEE + (TERM2/2.0)*(STRAN(I1) + .5*
     1         DSTRAN(I1))*DSTRAN(I1)
      END DO
C
      SSE = SSE + DEE
      SCD = SCD + TDE - DEE
C
      DO I = 1,6
         STATEV(I) = SM1(I)
      END DO
C
      DO I = 1,6
```

```
          STATEV(I+6) = SM2(I)
        END DO
C
C
        RETURN
        END
C
C**************************************************************
C
        SUBROUTINE SDVINI(STATEV,COORDS,NSTATV,NCRDS,NOEL,NPT,
     1                    LAYER,KSPT)
        INCLUDE 'ABA_PARAM.INC'
C
        DIMENSION STATEV(NSTATV),COORDS(NCRDS)
C
        DO I = 1,12
          STATEV(I) = 0.
        END DO
C
        RETURN
        END
C
C**************************************************************
C
        SUBROUTINE MAXWEL(SM1OLD,SM2OLD,
     1                    SM1,SM2,SM3,
     2                    SM1DOT,SM2DOT,
     3                    DTIME,PROPS,NPROPS,STRAN,NTENS)
C
C  This subroutine updates the Maxwell element (deviatoric) stresses and
C  computes the stress rates
C
        INCLUDE 'ABA_PARAM.INC'
C
        DIMENSION PROPS(NPROPS),STRAN(NTENS),SD(6),
C       DIMENSION PROPS(NPROPS),STRAN(NTENS),SD(NTENS),
```

```
     1          SM1OLD(6),SM2OLD(6),
     2          SM1(6),SM2(6),
     3          SM1DOT(6),SM2DOT(6)
C
       SP = (STRAN(1) + STRAN(2) + STRAN(3))/3.0
C
       SD(1) = STRAN(1) - SP
       SD(2) = STRAN(2) - SP
       SD(3) = STRAN(3) - SP
       SD(4) = STRAN(4)
       SD(5) = STRAN(5)
       SD(6) = STRAN(6)
C
       DO I = 1,3
        SM1(I) = (SM1OLD(I) - 2.0*PROPS(2)*SD(I))*EXP(-DTIME/PROPS(4)) +
     1             2.0*PROPS(2)*SD(I)
        SM2(I) = (SM2OLD(I) - 2.0*PROPS(3)*SD(I))*EXP(-DTIME/PROPS(5)) +
     2             2.0*PROPS(3)*SD(I)
       END DO
C
       DO I = 4,6
          SM1(I) = (SM1OLD(I) - PROPS(2)*SD(I))*EXP(-DTIME/PROPS(4)) +
     1             PROPS(2)*SD(I)
          SM2(I) = (SM2OLD(I) - PROPS(3)*SD(I))*EXP(-DTIME/PROPS(5)) +
     2             PROPS(3)*SD(I)
       END DO
C
       DO I =1,6
          SM1DOT(I) = (SM1(I) - SM1OLD(I))/DTIME
          SM2DOT(I) = (SM2(I) - SM2OLD(I))/DTIME
       END DO
C
       RETURN
       END
```

A.2.2 UMAT with Four Maxwell Elements (N = 4)

```
C   ************************************************************************
*                                                                       *
C   *                            U M A T                            *
C   *                                                                       *
C   *      AN ABAQUS USER MATERIAL MODEL FOR 3D VISCOELASTICITY      *
C   * (BASED ON MAXWELL ELEMENTS IN PARALLEL WITH AN ELASTIC SPRING) *
C   *                                                                       *
C   *                  CE521: SOLID MECHANICS                       *
C   *                    HWK. ASSIGNMENT #2                         *
C   *                                                                       *
C   *  WRITTEN BY : Prof. R. M. Hackett - University of Mississippi  *
C   *                    DATE : SPRING 1999                         *
C   *  REVISED BY : CHRIS L. MULLEN- University of Mississippi       *
C   *                    DATE : SPRING 1999                         *
C   *                                                                       *
C   ************************************************************************
C234567890123456789012345678901234567890123456789012345678901234567890
        SUBROUTINE UMAT (STRESS,STATEV,DDSDDE,SSE,SPD,SCD,
     1 RPL,DDSDDT,DRPLDE,DRPLDT,
     2 STRAN,DSTRAN,TIME,DTIME,TEMP,DTEMP,PREDEF,DPRED,CMNAME,
     3 NDI,NSHR,NTENS,NSTATV,PROPS,NPROPS,COORDS,DROT,PNEWDT,
     4 CELENT,DFGRD0,DFGRD1,NOEL,NPT,LAYER,KSPT,KSTEP,KINC)
C
        INCLUDE 'ABA_PARAM.INC'
C
C
        CHARACTER*8 CMNAME
        DIMENSION STRESS(NTENS),STATEV(NSTATV),
     1 DDSDDE(NTENS,NTENS),DDSDDT(NTENS),DRPLDE(NTENS),
     2 STRAN(NTENS),DSTRAN(NTENS),TIME(2),PREDEF(1),DPRED(1),
     3 PROPS(NPROPS),COORDS(3),DROT(3,3),DFGRD0(3,3),DFGRD1(3,3)
       DIMENSION DSTRES(6),D(3,3)
C
C
```

```
C  PROPS(1) through PROPS(5) are shear modulus values in MPa
c       PROPS(1) = 6.14
c       PROPS(2) = 3.5
c       PROPS(3) = 1.16
c       PROPS(4) = 0.52
c       PROPS(5) = 0.33
C  PROPS(6) through PROPS(9) are relaxation times in seconds
c       PROPS(6) = 0.311
c       PROPS(7) = 3.35
c       PROPS(8) = 35.7
c       PROPS(9) = 370
C  PROPS(10) is the bulk modulus in MPa
c       PROPS(10) = 307
C  DIMENSION VARIABLES THAT ARE INTERNAL TO SUBROUTINE
C
        DIMENSION SM1OLD(6),SM2OLD(6),SM3OLD(6),SM4OLD(6),
     1           SM1(6),SM2(6),SM3(6),SM4(6),
     2           SM1DOT(6),SM2DOT(6),SM3DOT(6),SM4DOT(6)
C
C
       WRITE(6,*)'THIS IS A TEST'
       WRITE(6,*) NDI, NSHR, NTENS, NSTATV, NPROPS
C
       DO I = 1,6
          SM1OLD(I) = STATEV(I)
       END DO
C
       DO I = 1,6
          SM2OLD(I) = STATEV(I+6)
       END DO
C
       DO I = 1,6
          SM3OLD(I) = STATEV(I+12)
C
       END DO
C
```

```
      DO I = 1,6
         SM4OLD(I) = STATEV(I+18)
      END DO
C
      GM = PROPS(1) + PROPS(2) + PROPS(3) +
     *     PROPS(4) + PROPS(5)
C  EVALUATE NEW STRESS TENSOR
      EV = 0.
      DEV = 0.
C
      DO K1 = 1,NDI
         EV = EV + STRAN(K1)
         DEV = DEV + DSTRAN(K1)
      END DO
C
      CALL MAXWEL(SM1OLD,SM2OLD,SM3OLD,SM4OLD,
     1            SM1,SM2,SM3,SM4,
     2            SM1DOT,SM2DOT,SM3DOT,SM4DOT,
     3            DTIME,PROPS,NPROPS,STRAN,NTENS)
C
      TERM1 = PROPS(10) - 2.0*GM/3.0
      TERM2 = 2.0*GM
C
      DO K1 = 1,NDI
         DSTRES(K1) = TERM1*DEV + TERM2*DSTRAN(K1) -
     1                2.0*(PROPS(6)*SM1DOT(K1) +
     2                     PROPS(7)*SM2DOT(K1) +
     3                     PROPS(8)*SM3DOT(K1) +
C
     4                     PROPS(9)*SM4DOT(K1)) +
     5               2.0*TERM1*EV + 2.0*TERM2*STRAN(K1) - 2.0*STRESS(K1)
         STRESS(K1) = STRESS(K1) + DSTRES(K1)
      END DO
C
      WRITE(6,1000) (STRESS(i),i=1,NDI)
 1000 FORMAT(6(1pe12.3))
```

```
c      STOP
       I1 = NDI
C
       DO K1 = 1,NSHR
          I1 = I1 + 1
          DSTRES(I1) = (TERM2/2.0)*DSTRAN(I1) -
     1                  2.0*(PROPS(6)*SM1DOT(I1) +
     2                      PROPS(7)*SM2DOT(I1) +
     3                      PROPS(8)*SM3DOT(I1) +
     4                      PROPS(9)*SM4DOT(I1)) +
     5                 2.0*(TERM2/2.0)*STRAN(I1) - 2.0*STRESS(I1)
          STRESS(I1) = STRESS(I1) + DSTRES(I1)
       END DO
C  CREATE NEW JACOBIAN
       DO K1 = 1,NTENS
          DO K2 = 1,NTENS
             DDSDDE(K2,K1) = 0.
          END DO
       END DO
C
       DO K1 = 1,NDI
          DDSDDE(K1,K1) = TERM1 + TERM2
       END DO
C
       DO K1 = 2,NDI
          N2 = K1 - 1
C
          DO K2 = 1,N2
             DDSDDE(K2,K1) = TERM1
             DDSDDE(K1,K2) = TERM1
          END DO
       END DO
C
       I1 = NDI
C
       DO K1 = 1,NSHR
```

```
          I1 = I1 + 1
          DDSDDE(I1,I1) = TERM2/2.0
       END DO
C
C  COMPUTE CHANGE IN SPECIFIC TOTAL ENERGY
C
       TDE = 0.
C
       DO K1 = 1,NTENS
          TDE = TDE + (STRESS(K1) + .5*DSTRES(K1))*
     1          DSTRAN(K1)
       END DO
C  COMPUTE CHANGE IN SPECIFIC ELASTIC STRAIN ENERGY
C
       DO K1 = 1,NDI
          D(K1,K1) = TERM1 + TERM2
       END DO
C
C
       DO K1 = 2,NDI
          N2 = K1 - 1
          DO K2 = 1,N2
             D(K1,K2) = TERM1
             D(K2,K1) = TERM1
          END DO
       END DO
C
       DEE = 0.
C
       DO K1 = 1,NDI
          TERM1 = 0.
          TERM2 = 0.
          DO K2 = 1,NDI
             TERM1 = TERM1 + D(K1,K2)*STRAN(K2)
             TERM2 = TERM2 + D(K1,K2)*DSTRAN(K2)
          END DO
```

```
          DEE = DEE + (TERM1 + .5*TERM2)*DSTRAN(K1)
        END DO
        I1 = NDI
        DO K1 = 1,NSHR
          I1 = I1 + 1
          DEE = DEE + (TERM2/2.0)*(STRAN(I1) + .5*
     1          DSTRAN(I1))*DSTRAN(I1)
        END DO
        SSE = SSE + DEE
        SCD = SCD + TDE - DEE
C
        DO I = 1,6
          STATEV(I) = SM1(I)
        END DO
C
        DO I = 1,6
          STATEV(I+6) = SM2(I)
        END DO
C
        DO I = 1,6
          STATEV(I+12) = SM3(I)
        END DO
C
        DO I = 1,6
          STATEV(I+18) = SM4(I)
        END DO
C
        RETURN
        END
C**********************************************************************
C
        SUBROUTINE SDVINI(STATEV,COORDS,NSTATV,NCRDS,NOEL,NPT,
     1                    LAYER,KSPT)
        INCLUDE 'ABA_PARAM.INC'
C
        DIMENSION STATEV(NSTATV),COORDS(NCRDS)
```

```
C
       DO I = 1,24
          STATEV(I) = 0.
       END DO
C
       RETURN
       END
C**********************************************************************
       SUBROUTINE MAXWEL(SM1OLD,SM2OLD,SM3OLD,SM4OLD,
     1                   SM1,SM2,SM3,SM4,
     2                   SM1DOT,SM2DOT,SM3DOT,SM4DOT,
     3                   DTIME,PROPS,NPROPS,STRAN,NTENS)
C  This subroutine updates the Maxwell element (deviatoric) stresses and
C  computes the stress rates
C
       INCLUDE 'ABA_PARAM.INC'
       DIMENSION PROPS(NPROPS),STRAN(NTENS),SD(6),
C                  DIMENSION PROPS(NPROPS),STRAN(NTENS),SD(NTENS),
     1           SM1OLD(6),SM2OLD(6),SM3OLD(6),SM4OLD(6),
     2           SM1(6),SM2(6),SM3(6),SM4(6),
     3           SM1DOT(6),SM2DOT(6),SM3DOT(6),SM4DOT(6)
C
       SP = (STRAN(1) + STRAN(2) + STRAN(3))/3.0
C
       SD(1) = STRAN(1) - SP
       SD(2) = STRAN(2) - SP
       SD(3) = STRAN(3) - SP
       SD(4) = STRAN(4)
       SD(5) = STRAN(5)
       SD(6) = STRAN(6)
C
       DO I = 1,3
        SM1(I) = (SM1OLD(I) - 2.0*PROPS(2)*SD(I))*EXP(-DTIME/PROPS(6)) +
     1             2.0*PROPS(2)*SD(I)
        SM2(I) = (SM2OLD(I) - 2.0*PROPS(3)*SD(I))*EXP(-DTIME/PROPS(7)) +
     2             2.0*PROPS(3)*SD(I)
```

```
         SM3(I) = (SM3OLD(I) - 2.0*PROPS(4)*SD(I))*EXP(-DTIME/PROPS(8)) +
     3             2.0*PROPS(4)*SD(I)
         SM4(I) = (SM4OLD(I) - 2.0*PROPS(5)*SD(I))*EXP(-DTIME/PROPS(9)) +
     4             2.0*PROPS(5)*SD(I)
       END DO
C
       DO I = 4,6
          SM1(I) = (SM1OLD(I) - PROPS(2)*SD(I))*EXP(-DTIME/PROPS(6)) +
     1             PROPS(2)*SD(I)
          SM2(I) = (SM2OLD(I) - PROPS(3)*SD(I))*EXP(-DTIME/PROPS(7)) +
     2             PROPS(3)*SD(I)
          SM3(I) = (SM3OLD(I) - PROPS(4)*SD(I))*EXP(-DTIME/PROPS(8)) +
     3             PROPS(4)*SD(I)
          SM4(I) = (SM4OLD(I) - PROPS(5)*SD(I))*EXP(-DTIME/PROPS(9)) +
     4             PROPS(5)*SD(I)
       END DO
C
       DO I =1,6
          SM1DOT(I) = (SM1(I) - SM1OLD(I))/DTIME
          SM2DOT(I) = (SM2(I) - SM2OLD(I))/DTIME
          SM3DOT(I) = (SM3(I) - SM3OLD(I))/DTIME
          SM4DOT(I) = (SM4(I) - SM4OLD(I))/DTIME
       END DO
C
       RETURN
       END
```

A.3 "SIGINI" Subroutine

This is the subroutine to include the pre-stress in the model.

```
C**********************************************************************
      SUBROUTINE SIGINI(SIGMA,COORDS,NTENS,NCRDS,NOEL,NPT,LAYER,
     1 KSPT,LREBAR,NAMES)

      INCLUDE 'ABA_PARAM.INC'
C
      DIMENSION SIGMA(NTENS),COORDS(NCRDS)
      CHARACTER NAMES(2)*80
      SIGMA(1) = -0.0855
      SIGMA(2) = 0.0855
      RETURN
      END
C**********************************************************************
```

Bibliography

[1] M. Wissler and E. Mazza, "Electromechanical coupling in dielectric elastomer actuators," *Sensors and Actuators A: Physical*, vol. 138, no. 2, pp. 384–393, 2007.

[2] X. Zhao and Z. Suo, "Method to analyze programmable deformation of dielectric elastomer layers," *Applied Physics Letters*, vol. 93, no. 25, p. 251902, 2008.

[3] A. Vinogradov, J. Su, C. Jenkins, and Y. Bar-Cohen, "State-of-the-art developments in the field of electroactive polymers," in *Material Research Society Symposium Proceedings*, vol. 889, pp. 51–56, 2006.

[4] G. Kofod and P. Sommer-Larsen, "Some aspects of large strain actuation in dielectric elastomers," in *12th International Symposium on Electrets*, pp. 208–211, 2005.

[5] Y. Bar-Cohen, "Electro-active polymers: current capabilities and challenges," in *Proceedings of the SPIE Smart Structures and Materials Symposium, EAPAD Conference, SanDiego, CA*, vol. 4695, pp. 1–7, March 2002.

[6] N. Goulbourne, E. Mockensturm, and M. Frecker, "A nonlinear model for dielectric elastomer membranes," *Journal of Applied Mechanics*, vol. 72, pp. 899–906, 2005.

[7] M. T. Wissler, *Modeling Dielectric Elastomer Actuators*. PhD thesis, Swiss Federal Institute Of Technology, Zurich, 2007.

[8] A. Wineman, "Nonlinear viscoelastic solids–a review," *Mathematics and Mechanics of Solids*, vol. 14, no. 3, pp. 300–366, 2009.

[9] A. V. Tobolsky and R. D. Andrews, "Systems manifesting superposed elastic and viscous behavior," *The Journal of Chemical Physics*, vol. 13, no. 1, pp. 3–27, 1945.

[10] Y. M. Haddad, *Viscoelasticity of engineering materials*, p. xix. Chapman & Hall, 1995.

[11] H. Zhang and L. Li, "Modeling inclusion problems in viscoelastic materials with the extended finite element method," *Finite Elements in Analysis and Design*, vol. 45, no. 10, pp. 721–729, 2009.

[12] Wikipedia, "Viscoelasticity." `http://en.wikipedia.org/wiki/Viscoelasticity`, October 2009.

[13] L. Boltzmann, "Zur theorie der elastischen nachwirkung," *In:(Sec. Ed. ed.), Mathematisch - Naturwissenschaftliche Classe*, vol. 70, pp. 275–306, 1874.

[14] M. Kaliske and H. Rothert, "Formulation and implementation of three-dimensional viscoelasticity at small and finite strains," *Computational Mechanics*, vol. 19, no. 3, pp. 228–239, 1997.

[15] A. Kaye *College of Aeronautics*, no. 134, 1962.

[16] B. Bernstein, E. A. Kearsley, and L. J. Zapas, "A study of stress relaxation with finite strain," *Transactions of the Society of Rheology*, no. 7, pp. 391–410, 1963.

[17] W. T. Read, Jr., "Stress analysis for compressible viscoelastic materials," *Journal of Applied Physics*, vol. 21, pp. 671–674, 1950.

[18] E. H. Lee, "Stress analysis in viscoelastic materials," *Journal of Applied Physics*, vol. 27, no. 7, pp. 665–672, 1956.

[19] E. H. Lee, "Stress analysis for linear viscoelastic materials," *Rheologica Acta*, vol. 1, pp. 426–430, 1961.

[20] B. D. Coleman and W. Noll, "Foundations of linear viscoelasticity," *Review of Modern Physics*, vol. 33, no. 2, pp. 239–249, 1961.

[21] A. C. Pipkin, "Small finite deformations of viscoelastic solids," *Review of Modern Physics*, 1964.

[22] A. Green and R. S. Rivlin, "The mechanics of non-linear materials with memory part i," *Archive for Rational Mechanics and Analysis*, vol. 1, no. 1, pp. 1 – 21, 1957.

[23] W. Noll, "A mathematical theory of the mechanical behavior of continuous media," *Archive for Rational Mechanics and Analysis*, vol. 2, no. 1, pp. 197–226, 1958.

[24] O. Zienkiewicz, M. Watson, and I. King, "A numerical method of visco-elastic stress analysis," *International Journal of Mechanical Sciences*, 1968.

[25] R. L. Taylor, K. S. Pister, and G. L. Goudreau, "Thermomechanical analysis of viscoelastic solids," *International Journal for Numerical Methods in Engineering*, vol. 2, no. 1, pp. 45–59, 1970.

[26] A. C. Pipkin and T. G. Rogers, "A non-linear integral representation for viscoelastic behaviour," *Journal of the Mechanics and Physics of Solids*, vol. 16, no. 1, pp. 59–72, 1968.

[27] R. A. Schapery, "On the characterization of nonlinear viscoelastic materials," *Polymer Engineering & Science*, vol. 9, no. 4, pp. 295–310, 1969.

[28] Y. Partom and I. Schanin, "Modeling nonlinear viscoelastic response," *Polymer Engineering & Science*, vol. 23, no. 15, pp. 849–859, 1983.

[29] B. Keren, Y. Partom, and Z. Rosenberg, "Nonlinear viscoelastic response in two dimensions - numerical modeling," *Polymer Engineering & Science*, vol. 24, no. 18, pp. 1409–1416, 1984.

[30] R. W. Rendell, K. L. Ngai, G. R. Fong, A. F. Yee, and R. J. Bankert, "Nonlinear viscoelasticity and yield: Application of a coupling model," *Polymer Engineering & Science*, vol. 27, no. 1, pp. 2–15, 1987.

[31] K. C. Gramoll, D. A. Dillard, and H. F. Brinson, "A stable numerical solution method for in-plane loading of nonlinear viscoelastic laminated orthotropic materials," *Composite Structures*, vol. 13, no. 4, pp. 251–274, 1989.

[32] P. Krishnaswamy, M. E. Tuttle, A. F. Emery, and J. Ahmad, "Finite element modelling of crack tip behaviour in viscoelastic materials. part i: Linear behaviour," *International Journal for Numerical Methods in Engineering*, vol. 30, no. 2, pp. 371–387, 1990.

[33] G. U. Losi and W. G. Knauss, "Thermal stresses in nonlinearly viscoelastic solids," *Journal of Applied Mechanics*, vol. 59, no. 25, pp. S43–S49, 1992.

[34] G. Ghazlan, S. Caperaa, and C. Petit, "An incremental formulation for the linear analysis of thin viscoelastic structures using generalized variables," *International Journal for Numerical Methods in Engineering*, vol. 38, no. 19, pp. 3315–3333, 1995.

[35] S. P. Zaoutsos, G. C. Papanicolaou, and A. H. Cardon, "On the non-linear viscoelastic behaviour of polymer-matrix composites," *Composites Science and Technology*, vol. 58, no. 6, pp. 0266–3538, 1998.

[36] S. Reese and S. Govindjee, "Theoretical and numerical aspects in the thermo-viscoelastic material behaviour of rubber-like polymers," *Mechanics of Time-Dependent Materials*, vol. 1, no. 4, pp. 357–396, 1997.

[37] J. R. Masuero and G. J. Creus, "Finite elements analysis of viscoelastic fracture," *International Journal of Fracture*, vol. 60, no. 3, pp. 267–282, 1993.

[38] C. S. Drapaca, S. Sivaloganathan, and G. Tenti, "Nonlinear constitutive laws in viscoelasticity," *Mathematics and Mechanics of Solids*, vol. 12, no. 5, pp. 475–501, 2007.

[39] R. S. Lakes, *Viscoelastic Solids*, ch. 6. CRC Press, October 1998.

[40] Wikipedia, "Viscoelasticity." `http://en.wikipedia.org/wiki/Creep_(deformation)`, October 2009.

[41] D. V. Rosato, D. V. Rosato, and M. Rosato, *Plastics Design Handbook*. Springer - Verlag, 2001.

[42] Instron, "Creep and stress-relaxation test." `http://www.instron.us/wa/applications/test_types/creep_stress_relax.aspx`, April 2010.

[43] Y. Bar-Cohen, ed., *Electroactive Polymer (EAP) Actuators as Artificial Muscles: Reality, Potential, and Challenges*. SPIE Publications, second ed., 2004.

[44] J. C. Koo, K.-M. Jung, M.-Y. Jung, H. Choi, J. Nam, and Y. Lee, "Effect of pre-strain on the antagonistically driven dielectric polymer actuator," *Key Engineering Materials*, vol. 306/308; Part 2, pp. 1187–1192, 2006.

[45] J. W. Fox, "Electromechanical characterization of the static and dynamic response of dielectric elastomer membranes," Master's thesis, Virginia Polytechnic Institute and State University, Blacksburg, Virginia, 2007.

[46] E. Biddiss and T. Chaua, "Dielectric elastomers as actuators for upper limb prosthetics: Challenges and opportunities," *Medical Engineering & Physics*, vol. 30, no. 4, pp. 403–418, 2008.

[47] R. Shankar, T. K. Ghosh, and R. J. Spontak, "Dielectric elastomers as next-generation polymeric actuators," *Soft Matter*, vol. 3, pp. 1116–1129, 2007.

[48] M. Wissler and E. Mazza, "Modeling and simulation of dielectric elastomer actuators," *Smart Mater. Struct.*, vol. 14, no. 6, pp. 1396–1402, 2005.

[49] J. Fox and N. Goulbourne, "On the dynamic electromechanical loading of dielectric elastomer membranes," *Journal of the Mechanics and Physics of Solids*, vol. 56, no. 8, pp. 2669–2686, 2008.

[50] H. Wang, J. Zhu, and K. Ye, "Simulation, experimental evaluation and performance improvement of a cone dielectric elastomer actuator," *Journal of Zhejiang University SCIENCE A*, vol. 10, no. 9, pp. 1296–1304, 2009.

[51] P. Lochmatter, G. Kovacs, and S. Michel, "Characterization of dielectric elastomer actuators based on a hyperelastic film model," *Sensors and Actuators A: Physical*, vol. 135, no. 2, pp. 748–757, 2007.

[52] O. Yeoh, "Characterization of elastic properties of carbon-black-filled rubber vulcanizates," *Rubber Chem. Technol.*, vol. 63, pp. 792–805, 1990.

[53] H. R. Choi, K. Jung, S. Ryew, J.-D. Nam, J. Jeon, J. C. Koo, and K. Tanie, "Biomimetic soft actuator: Design, modeling, control, and applications," *IEEE/ASME TRANSACTIONS ON MECHATRONICS*, vol. 10, no. 5, pp. 581–593, 2005.

[54] M. R. Begley, H. Bart-Smith, O. N. Scott, M. H. Jones, and M. L. Reed, "The electro-mechanical response of elastomer membranes coated with ultra-thin metal electrodes," *Journal of the Mechanics and Physics of Solids*, 2005.

[55] M. R. Begley and T. J. Mackin, "Spherical indentation of freestanding circular thin films in the membrane regime," *Journal of the Mechanics and Physics of Solids*, vol. 52, no. 9, pp. 2005 – 2023, 2004.

[56] F. Carpi and D. D. Rossi, "Biomimetic dielectric elastomer actuators," in *Biomedical Robotics and Biomechatronics, 2006. BioRob 2006. The First IEEE/RAS-EMBS International Conference on*, pp. 1073–1078, 2006.

[57] E. M. Mockensturm and N. Goulbourne, "Dynamic response of dielectric elastomers," *International Journal of Non-Linear Mechanics*, vol. 41, no. 3, pp. 388–395, 2006.

[58] J.-S. Plante and S. Dubowsky, "On the properties of dielectric elastomer actuators and their design implications," *Smart Materials and Structures*, vol. 16, no. 2, pp. 227–236, 2007.

[59] R. E. Pelrine, R. D. Kornbluh, and J. P. Joseph, "Electrostriction of polymer dielectrics with compliant electrodes as a means of actuation," *Sensors and Actuators A: Physical*, vol. 64, no. 1, pp. 77 – 85, 1998. Tenth IEEE International Workshop on Micro Electro Mechanical Systems.

[60] J.-S. Plante and S. Dubowsky, "On the performance mechanisms of dielectric elastomer actuators," *Sensors and Actuators A: Physical*, vol. 137, no. 1, pp. 96–109, 2007.

[61] J. Fox and N. Goulbourne, "Electric field-induced surface transformations and experimental dynamic characteristics of dielectric elastomer membranes," *Journal of the Mechanics and Physics of Solids*, vol. 57, no. 8, pp. 1417–1435, 2009.

[62] A. Green and J. Adkins, *Large Elastic Deformations*. Oxford University Press, London, 1970.

[63] R. Shankar, T. K. Ghosh, and R. J. Spontak, "Mechanical and actuation behavior of electroactive nanostructured polymers," *Sensors and Actuators A: Physical*, vol. 151, no. 1, pp. 46–52, 2009.

[64] F. Carpi, D. D. Rossi, R. Kornbluh, R. Pelrine, and P. Sommer-Larsen, eds., *Dielectric Elastomers as Electromechanical Transducers*, ch. V. Fundamentals, Materials, Devices, Models and Applications of an Emerging Electroactive Polymer Technology, Elsevier Ltd., 2008.

[65] O. Zienkiewicz and R. Taylor, *The Finite Element Method for Solid and Structural Mechanics*. Elsevier Butterworth-Heinemann, sixth ed., 2005.

[66] J. Bonet and R. D. Wood, *Nonlinear Continuum Mechanics for Finite Element Analysis*. Cambridge University Press, 1997.

[67] G. Mase, *Schaum's Outline of Continuum Mechanics*. McGraw-Hill, 1969.

[68] G. A. Holzapfel, *Nonlinear Solid Mechanics: A Continuum Approach for Engineering*. Wiley, first ed., 2000.

[69] J. Simo and T. Hughes, *Computational Inelasticity*. Springer, 1998.

[70] T. Belytschko, W. K. Liu, and B. Moran, *Nonlinear Finite Elements for Continua and Structures*. Wiley, first ed., 2000.

[71] Dassault Systèmes Simulia Corp., Providence, RI, USA, *Abaqus User Subroutines Reference Manual*, 2009.

[72] Dassault Systèmes Simulia Corp., Providence, RI, USA, *Abaqus Analysis User's Manual*, 2009.

[73] Dassault Systèmes Simulia Corp., Providence, RI, USA, *Abaqus Verification Manual*, 2009.

[74] R. M. Hackett, "An abaqus user material model for 3d viscoelasticity." `http://www.olemiss.edu/courses/ce521/f77.html`, 1999. University of Mississippi.